Article

# Discovery of Carboline Derivatives as Potent Antifungal Agents for the Treatment of Cryptococcal Meningitis

Jie Tu, Zhuang Li, Yanjuan Jiang, Changjin Ji, Guiyan Han, Yan Wang, Na Liu, and Chunquan Sheng

## Just Accepted

1
2
3
4
5
6
7
8
9
10
11
12
13
14
15
16
17
18
19
20
21
22
23
24
25
26
27
28
29
30
31
32
33
34
35
36
37
38
39
40
41
42
43
44
45
46
47
48
49
50
51
52
53
54
55
56
57
58
59
60

# Discovery of Carboline Derivatives as Potent Antifungal Agents for the Treatment of Cryptococcal Meningitis

Jie Tu[†], Zhuang Li[†], Yanjuan Jiang, Changjin Ji, Guiyan Han, Yan Wang, Na Liu*,

Chunquan Sheng*

*Department of Medicinal Chemistry, School of Pharmacy, Second Military Medical*

*University, 325 Guohe Road, Shanghai 200433, People's Republic of China*

1

**ABSTRACT**

Clinical treatment of cryptococcal meningitis (CM) remains a significant challenge due to the lack of effective and safe drug therapies. Developing novel CM therapeutic agents with novel chemical scaffolds and new modes of action is of great importance. Herein, new *β*-hexahydrocarboline derivatives were shown to possess potent anticryptococcal activities. In particular, compound **A4** showed potent *in vitro* and *in vivo* anticryptococcal activity with good metabolic stability and BBB permeability. Compound **A4** was orally active and could significantly reduce brain fungal burdens in a murine model of CM. Moreover, compound **A4** could inhibit several virulence factors of *C. neoformans* and might act by a new mode of action. Preliminary mechanistic studies revealed that compound **A4** induced DNA double stranded breaks and cell cycle arrest at the G2 phase by acting on the Cdc25c/CDK1/cyclin B pathway. Taken together, *β*-hexahydrocarboline **A4** represents a promising lead compound for the development of next-generation CM therapeutic agents.

**INTRODUCTION**

The clinical treatment of life-threatening invasive fungal infections (IFIs) remains a significant global challenge.[1, 2] Species of *Candida, Cryptococcus, Aspergillus*, and *Pneumocystis* are major fungal pathogens accounting for nearly 90% of lethal cases in humans.[3] *Cryptococcus neoformans (C. neoformans var. grubii* and *C. neoformans var. neoformans)* and *Cryptococcus gattii* are responsible for most cases of fungal meningitis worldwide.[4, 5] Cryptococcal meningitis (CM), one of the most important lethal factors in HIV/AIDS patients, is always fatal if left untreated.[5-7] Clinically, antifungal agents for the treatment of CM mainly include polyenes (*e.g.,* liposomal or deoxycholate amphotericin B), nucleic acid analogues (*e.g.,* 5-flucytosine), and azoles (*e.g.,* fluconazole (FLC)).[8] However, amphotericin B, the drug with the greatest early fungicidal activity (EFA), is associated with renal impairment.[9] Toxic cytopenias can occur during 5-flucytosine therapy, and thus regular full blood counts and therapeutic drug monitoring (TDM) are advised. FLC is fungistatic rather than fungicidal in the normal human dose range, and it is therefore often used as a maintenance therapy.[4] The newly developed *β*-1,3-glucan synthase inhibitors (i.e., echinocandins) are ineffective against *Cryptococcus* species.[10, 11] The current "gold standard" for the treatment of CM is still based on a combination of amphotericin B and 5-flucytosine that was developed more than 50 years ago.[11] Currently, 5-fluorocytosine remains unlicensed in most African and Asian countries.[4, 12] Despite the increasing clinical demands, the development of new drugs for the treatment of CM has been relatively slow. In recent years, the search for anticryptococcal agents has mainly focused on

drug repurposing and alternative preparations of the "gold standard" mixture.[3, 13-16] The discovery of new molecules to treat cryptococcal infections remains quite challenging. Therefore, developing novel CM therapeutic agents with novel chemical scaffolds and new modes of action is of great importance.[17]

Previously, our group identified γ-hexahydrocarboline scaffold **1** as a new antifungal scaffold by screening against an in-house library.[18] Further structural optimization led to γ-tetrahydrocarboline **2 (C38),** which showed improved antifungal activity. Its activity was comparable to that of FLC but without toxicity to human embryonic lung cells.[18] In particular, carboline **2** showed features that suggested it could overcome the drug resistance of FLC. For example, it exhibited good antifungal activity against both FLC-sensitive and FLC-resistant *C. albicans* cells and had potent inhibitory activity against *C. albicans* biofilm formation and hyphal growth. Moreover, the anticryptococcal activity of compound **2** (*C. neoformans*, $MIC_{80} = 1$ μg/mL) was also better than that of compound **1** (*C. neoformans*, $MIC_{80} = 8$ μg/mL, **Figure 1**). However, based on further studies, the development of γ-tetrahydrocarbolines was hampered by their poor *in vivo* potency.

A series of *β*-carboline derivatives based on γ-carboline **2** were designed and synthesized, and they showed increased anticryptococcal activities (**Figure 1** and **Figure S1** in the Supporting Information). In particular, compound **A4** showed strong *in vitro* and *in vivo* anticryptococcal activities, making it a promising lead compound for the development of novel anticryptococcal agents. Preliminary studies on the anticryptococcal mechanism of **A4** indicated that it might act by a new mode of

4

action.
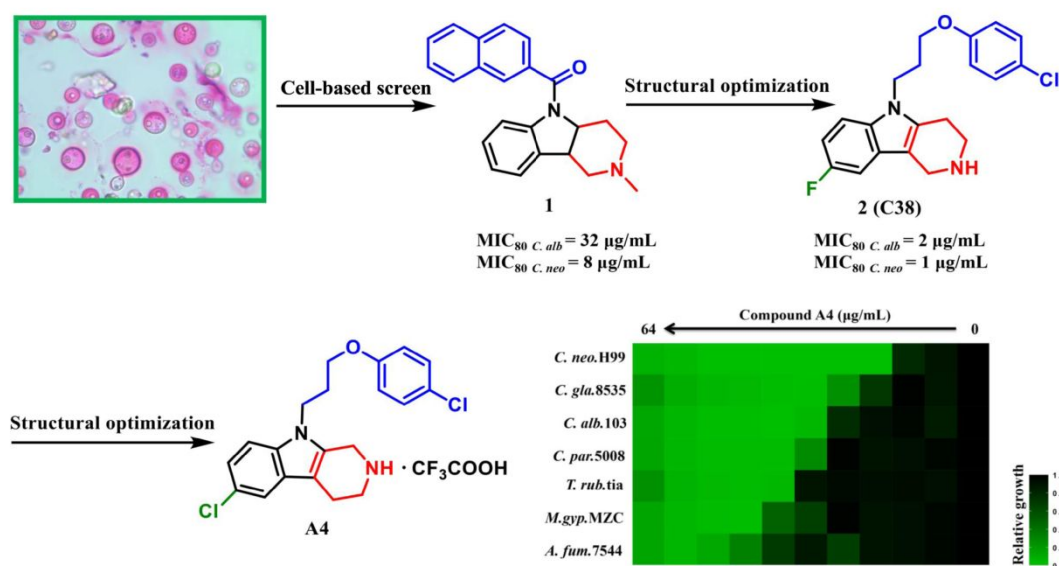


**Figure 1**. Discovery and structural optimization of carboline-based antifungal compounds. The minimum inhibitory concentration (MIC) was measured by the optical density at 600 nm (OD600), and the relative growth is displayed as a heatmap. Abbreviations: *C. alb. Candida albicans; C. par. Candida parapsilosis; C. neo. Cryptococcus neoformans; C. gatti. Cryptococcus gattii; C. gla. Candida glabrata; A. fum. Aspergillus fumigatus; T. rub. Trichophyton rubrum; M. gyp. Microsporum gypseum.*

## CHEMISTRY

The chemical syntheses of the *β*-tetrahydrocarboline derivatives are depicted in **Schemes 1-4.** Intermediates **5a-q** were synthesized from commercially available substituted tryptamines via two steps according to the reported methods.[19] Reacting 1,3-dibromopropanes (**3a-o**) with the appropriately substituted phenols in the presence

5

of $K_2CO_3$ and ethanol gave intermediates **4a-o**, which were reacted with intermediates

**5a-q** to form compounds **6**. Finally, the Boc protecting groups were removed under

acidic conditions (trifluoroacetate (TFA)) to afford substituted *β*-tetrahydrocarboline

derivatives **A1-30** (**Scheme 1**).

**Scheme 1**



| | | | |
|---|---|---|---|
| **3, 4a** $R_2$ = 4'-Cl | **3, 4i** $R_2$ = 3'-OCH$_3$ | | |
| **3, 4b** $R_2$ = 2'-F | **3, 4j** $R_2$ = 4'-F | | |
| **3, 4c** $R_2$ = 2'-Cl | **3, 4k** $R_2$ = 4'-Br | | |
| **3, 4d** $R_2$ = 2'-Br | **3, 4l** $R_2$ = 4'-CH$_3$ | | |
| **3, 4e** $R_2$ = 2'-OCH$_3$ | **3, 4m** $R_2$ = 4'-OCH$_3$ | | |
| **3, 4f** $R_2$ = 3'-F | **3, 4n** $R_2$ = 4'-NO$_2$ | | |
| **3, 4g** $R_2$ = 3'-Cl | **3, 4o** $R_2$ = 4'-Cl | | |
| **3, 4h** $R_2$ = 3'-Br | | | |

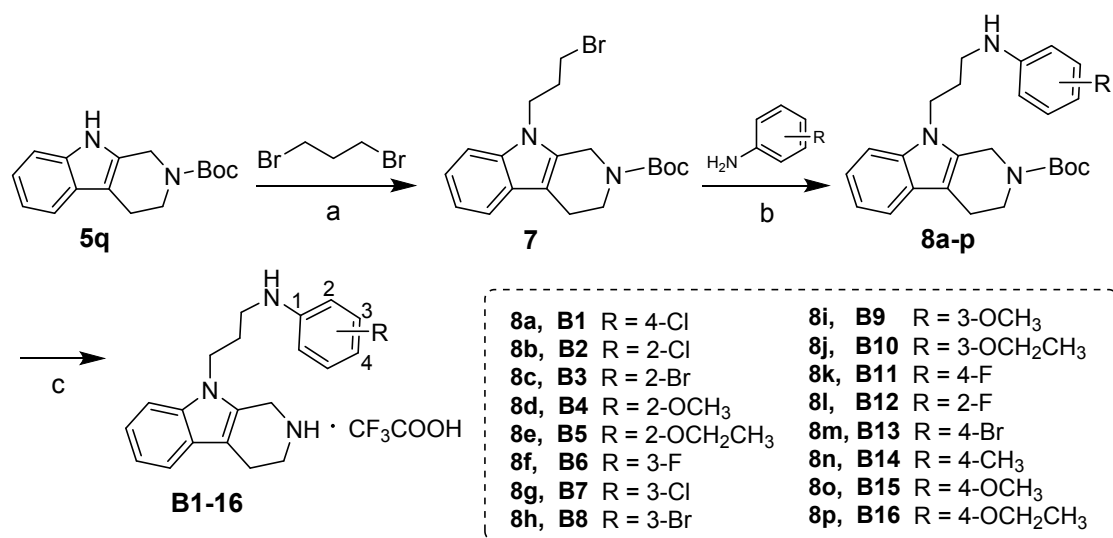| | |
|---|---|
| **5a** $R_1$ = 5-Br | **5j** $R_1$ = 7-Br |
| **5b** $R_1$ = 5-Cl | **5k** $R_1$ = 7-CH$_3$ |
| **5c** $R_1$ = 5-F | **5l** $R_1$ = 7-OCH$_3$ |
| **5d** $R_1$ = 6-Cl | **5m** $R_1$ = 8-Cl |
| **5e** $R_1$ = 6-Br | **5n** $R_1$ = 8-Br |
| **5f** $R_1$ = 6-CH$_3$ | **5o** $R_1$ = 8-CH$_3$ |
| **5g** $R_1$ = 6-OCH$_3$ | **5p** $R_1$ = 8-OCH$_3$ |
| **5h** $R_1$ = 7-F | **5q** $R_1$ = H |
| **5i** $R_1$ = 7-Cl | |

| | | | | |
|---|---|---|---|---|
| **A1** | $R_1$ = 5-Br | $R_2$ = 4'-Cl | **A16** $R_1$ = 8-OCH$_3$ | $R_2$ = 4'-Cl |
| **A2** | $R_1$ = 5-Cl | $R_2$ = 4'-Cl | **A17** $R_1$ = H | $R_2$ = 2'-F |
| **A3** | $R_1$ = 5-F | $R_2$ = 4'-Cl | **A18** $R_1$ = H | $R_2$ = 2'-Cl |
| **A4** | $R_1$ = 6-Cl | $R_2$ = 4'-Cl | **A19** $R_1$ = H | $R_2$ = 2'-Br |
| **A5** | $R_1$ = 6-Br | $R_2$ = 4'-Cl | **A20** $R_1$ = H | $R_2$ = 2'-OCH$_3$ |
| **A6** | $R_1$ = 6-CH$_3$ | $R_2$ = 4'-Cl | **A21** $R_1$ = H | $R_2$ = 3'-F |
| **A7** | $R_1$ = 6-OCH$_3$ | $R_2$ = 4'-Cl | **A22** $R_1$ = H | $R_2$ = 3'-Cl |
| **A8** | $R_1$ = 7-F | $R_2$ = 4'-Cl | **A23** $R_1$ = H | $R_2$ = 3'-Br |
| **A9** | $R_1$ = 7-Cl | $R_2$ = 4'-Cl | **A24** $R_1$ = H | $R_2$ = 3'-OCH$_3$ |
| **A10** | $R_1$ = 7-Br | $R_2$ = 4'-Cl | **A25** $R_1$ = H | $R_2$ = 4'-F |
| **A11** | $R_1$ = 7-CH$_3$ | $R_2$ = 4'-Cl | **A26** $R_1$ = H | $R_2$ = 4'-Br |
| **A12** | $R_1$ = 7-OCH$_3$ | $R_2$ = 4'-Cl | **A27** $R_1$ = H | $R_2$ = 4'-CH$_3$ |
| **A13** | $R_1$ = 8-Cl | $R_2$ = 4'-Cl | **A28** $R_1$ = H | $R_2$ = 4'-OCH$_3$ |
| **A14** | $R_1$ = 8-Br | $R_2$ = 4'-Cl | **A29** $R_1$ = H | $R_2$ = 4'-NO$_2$ |
| **A15** | $R_1$ = 8-CH$_3$ | $R_2$ = 4'-Cl | **A30** $R_1$ = H | $R_2$ = 4'-Cl |

**Reagents and conditions:** (a) $K_2CO_3$, EtOH, 80°C, 4 h, yield 51-66%; (b) NaH,

DMF, rt, 1 h, yield 34-54%; (c) TFA, $CH_2Cl_2$, rt, 0.5 h, yield 71-85%.

6

Compounds **B1-16** were synthesized according to the procedures outlined in

**Scheme 2**. Excess 1,3-dibromopropane was reacted with intermediate **5q** to give

compound **7**. Compound **7** was reacted with various substituted anilines in the

presence of KI, $K_2CO_3$ and MeCN to afford intermediates **8a-p**, which were further

deprotected in the presence of TFA to give target compounds **B1-16**. As shown in

**Scheme 3**, compounds **9a-l** were obtained by reacting intermediate **7** with various

amines in DMF. The Boc groups of compounds **9a-l** were removed under acidic

conditions (TFA), and then free amine **C1-12** were prepared under alkaline

conditions. Using a similar procedure, compounds **C13-14** were synthesized by

reacting intermediate **5q** with **10a-b** in the presence of NaOH and DMF followed by

Boc deprotection (**Scheme 4**).

**Scheme 2**



| | | | | |
|---|---|---|---|---|
| **8a, B1** | R = 4-Cl | | **8i, B9** | R = 3-OCH$_3$ |
| **8b, B2** | R = 2-Cl | | **8j, B10** | R = 3-OCH$_2$CH$_3$ |
| **8c, B3** | R = 2-Br | | **8k, B11** | R = 4-F |
| **8d, B4** | R = 2-OCH$_3$ | | **8l, B12** | R = 2-F |
| **8e, B5** | R = 2-OCH$_2$CH$_3$ | | **8m, B13** | R = 4-Br |
| **8f, B6** | R = 3-F | | **8n, B14** | R = 4-CH$_3$ |
| **8g, B7** | R = 3-Cl | | **8o, B15** | R = 4-OCH$_3$ |
| **8h, B8** | R = 3-Br | | **8p, B16** | R = 4-OCH$_2$CH$_3$ |

**Reagents and conditions:** (a) NaOH, DMF, rt, 1 h, yield 17-21%; (b) $K_2CO_3$, MeCN,

85°C, 1 h, yield 42-86%; (c) TFA, $CH_2Cl_2$, rt, 0.5 h, yield 37-80%.

**Scheme 3**
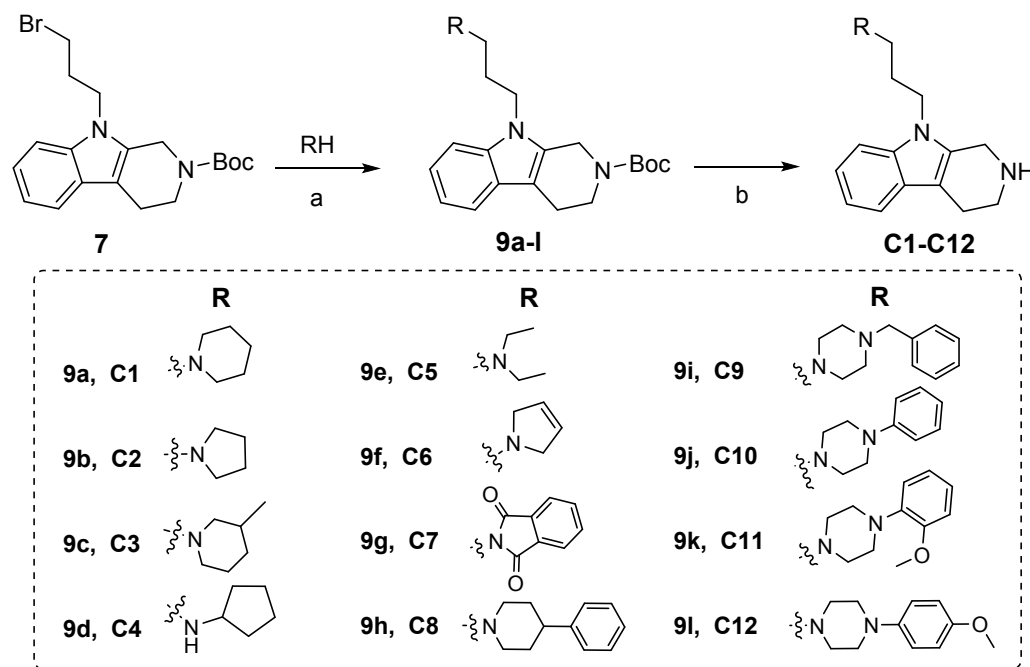


**Reagents and conditions:** (a) DMF, rt, 4 h, yield 13-91%; (b) TFA, $CH_2Cl_2$, rt, 0.5 h, yield 18-71%.

**Scheme 4**
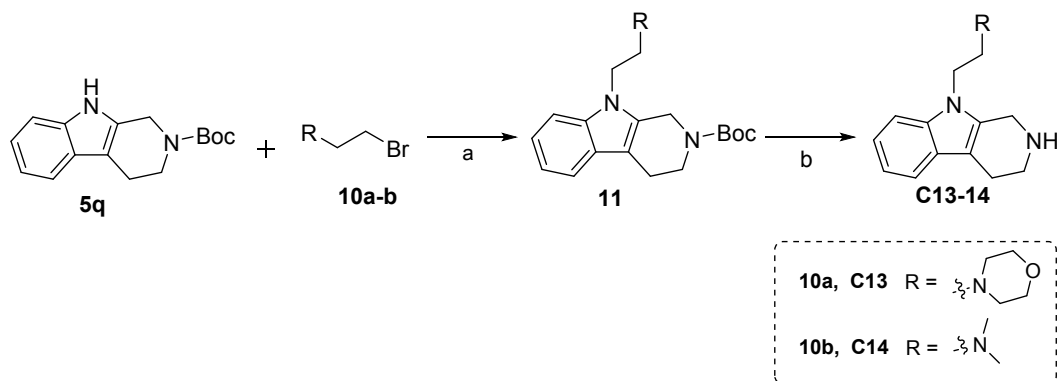


**Reagents and conditions:** (a) NaOH, DMF, rt, 1 h, yield 15-21%; (b) TFA, $CH_2Cl_2$, rt, 0.5 h, yield 45-76%.

8

## RESULTS AND DISCUSSION

**Anticryptococcal Activity and Structure−Activity Relationship**. A series of new carboline derivatives were designed and synthesized (**Schemes 1-4**). Their *in vitro* anticryptococcal activities are summarized in **Tables 1-3**. The antifungal activities are expressed as the MIC to achieve 80% inhibition of *C. neoformans*. The triazole-based antifungal drug FLC, used as the first-line therapy in the treatment of candidiasis and cryptococcosis, was chosen as the positive control. TFA itself has no antifungal activity (MIC > 64 μg/mL).

First, various substituents on the benzene ring of the tetrahydrocarboline scaffold (**A1-16**) and the terminal phenol group in the side chain (**A17-30**) were investigated. Generally, derivatives **A1-30** exhibited moderate to good antifungal activities against the *C. neoformans* H99 strain. Substitution at the C6 position was more favorable than at the C7, C8 and C5 positions, and a C6-chlorine group gave the best results. Among the tested substituents on the terminal benzene ring, halogen substituents provided better activity than methyl, alkoxyl and nitro substituents. Substitution at the C4' and C3' positions provided better results than substitution at the C2'. Interestingly, compound **A4**, the C6,C4'-dichloro derivative, showed excellent activity against *C. neoformans* ($MIC_{80}$ = 0.25 μg/mL at 48 h; $MIC_{80}$ = 0.5 μg/mL at 72 h), and it was more potent than FLC.

Second, the importance of the oxygen atom in the side chain (**B1-16**) was investigated. The replacement of the oxygen atom with a nitrogen atom led to a decrease in the antifungal activity. Consistent with the SAR in series A, compounds

with halogen substituents on the benzene ring of the side chain were more potent than the corresponding methyl and alkoxyl derivatives. Finally, substituted benzene rings were replaced by various aliphatic amines (**C1-C14**). However, an obvious decrease in the antifungal activities was observed for all of the aliphatic amine derivatives.

Among the target compounds, compounds **A4**, **A5** and **A6** showed potent anticryptococcal activities. Notably, the solubility assay revealed that **A4** (solubility: 54.6 μg/mL) and **A6** (solubility: 57.5 μg/mL) were significantly more soluble than **A5** (solubility: 19.3 μg/mL). Therefore, compounds **A4** and **A6** were chosen for further biological evaluations. An assay of the spectrum of the antifungal activity revealed that compounds **A4** and **A6** could inhibit a wide range of fungal pathogens, including *Candida albicans*, *Candida parapsilosis*, *Candida glabrata*, *Cryptococcus gattii*, *Aspergillus fumigates*, *Trichophyton rubrum* and *Microsporum gypseum* (**Table 4**). Moreover, both compounds showed high plasma protein binding and low toxicity to human HUVECs (**Tables S1** and **S2** in Supporting Information).

**Table 1.** *In vitro* antifungal activities of carboline derivatives A1-30 (MIC$_{80}$, µg/mL, 48 h)
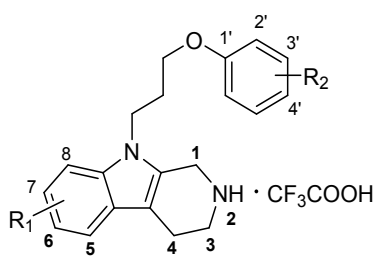
| Compds | R$_1$ | R$_2$ | C. neo. | Compds | R$_1$ | R$_2$ | C. neo. |
|--------|-------|-------|---------|--------|-------|-------|---------|
| A1 | 5-Br | 4'-Cl | 8 | A17 | H | 2'-F | 16 |
| A2 | 5-Cl | 4'-Cl | 4 | A18 | H | 2'-Cl | 4 |
| A3 | 5-F | 4'-Cl | 4 | A19 | H | 2'-Br | 8 |
| A4 | 6-Cl | 4'-Cl | 0.25 | A20 | H | 2'-OCH$_3$ | 32 |
| A5 | 6-Br | 4'-Cl | 0.5 | A21 | H | 3'-F | 8 |
| A6 | 6-CH$_3$ | 4'-Cl | 1 | A22 | H | 3'-Cl | 4 |
| A7 | 6-OCH$_3$ | 4'-Cl | 4 | A23 | H | 3'-Br | 4 |
| A8 | 7-F | 4'-Cl | 2 | A24 | H | 3'-OCH$_3$ | 16 |
| A9 | 7-Cl | 4'-Cl | 2 | A25 | H | 4'-F | 8 |
| A10 | 7-Br | 4'-Cl | 2 | A26 | H | 4'-Br | 4 |
| A11 | 7-CH$_3$ | 4'-Cl | 2 | A27 | H | 4'-CH$_3$ | 8 |
| A12 | 7-OCH$_3$ | 4'-Cl | 2 | A28 | H | 4'-OCH$_3$ | 16 |
| A13 | 8-Cl | 4'-Cl | 2 | A29 | H | 4'-NO$_2$ | 16 |
| A14 | 8-Br | 4'-Cl | 4 | A30 | H | 4'-Cl | 4 |
| A15 | 8-CH$_3$ | 4'-Cl | 2 | FLC | | | 4 |

| A16 | 8-OCH$_3$ | 4'-Cl | 4 | |
|---|---|---|---|---|
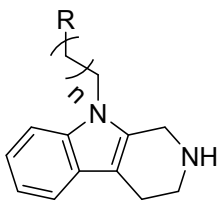
**Table 2.** *In vitro* **antifungal activities of the carboline derivatives B1-16 (MIC$_{80}$, μg/mL, 48 h)[a]**
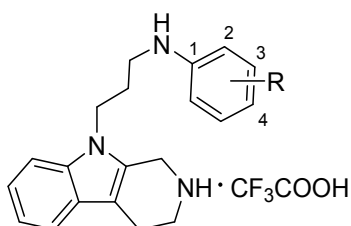


| Compds | R | *C. neo.* | Compds | R | *C. neo.* |
|---|---|---|---|---|---|
| **B1** | 4-Cl | 8 | **B10** | 3-OCH$_2$CH$_3$ | 64 |
| **B2** | 2-Cl | 8 | **B11** | 4-F | 16 |
| **B3** | 2-Br | 8 | **B12** | 2-F | 16 |
| **B4** | 2-OCH$_3$ | 32 | **B13** | 4-Br | 8 |
| **B5** | 2-OCH$_2$CH$_3$ | 32 | **B14** | 4-CH$_3$ | 16 |
| **B6** | 3-F | 16 | **B15** | 4-OCH$_3$ | 32 |
| **B7** | 3-Cl | 8 | **B16** | 4-OCH$_2$CH$_3$ | 32 |
| **B8** | 3-Br | 8 | **FLC** | | 4 |
| **B9** | 3-OCH$_3$ | 32 | | | |

12

1
2
3
4
5
6
7
8
9
10
11
12
13
14
15
16
17
18
19
20
21
22
23
24
25
26
27
28
29
30
31
32
33
34
35
36
37
38
39
40
41
42
43
44
45
46
47
48
49
50
51
52
53
54
55
56
57
58
59
60

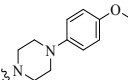**Table 3.** *In vitro* antifungal activities of carboline derivatives C1-14 (MIC$_{80}$, µg/mL, 48 h)[a]
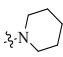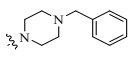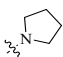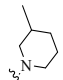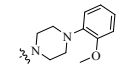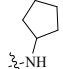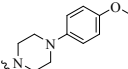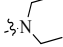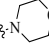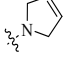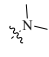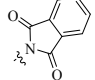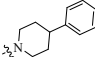


| Compds | R | n | *C. neo.* | Compds | R | n | *C. neo.* |
|---|---|---|---|---|---|---|---|
| **C1** | | 2 | 64 | **C9** | | 2 | 32 |
| **C2** | | 2 | 64 | **C10** | | 2 | 32 |
| **C3** | | 2 | 32 | **C11** | | 2 | 64 |
| **C4** | | 2 | 64 | **C12** | | 2 | 64 |
| **C5** | | 2 | 64 | **C13** | | 1 | 64 |
| **C6** | | 2 | 64 | **C14** | | 1 | 64 |
| **C7** | | 2 | 64 | **FLC** | | | 4 |
| **C8** | | 2 | 32 | | | | |

**Table 4.** *In vitro* antifungal activities of compounds A4 and A6

| Compds | MIC80, µg/mL, 48 h | | | | | | | MIC$_{80}$, µg/mL, 72 h | | |
|---|---|---|---|---|---|---|---|---|---|---|
| | *C. gla.* 8535 | *C. alb.* 7781 | *C. alb.* 0304103 | *C. par.* 5008 | *A. fum.* 7544 | *T. rub.* TIA | *M. gyp.* MZC | *C. neo.* H99 | *C. neo.* ATCC34877 | *C. gat.* ATCC14116 |
| **A4** | 1 | 4 | 2 | 2 | 16 | 4 | 8 | 0.5 | 0.5 | 1 |
| **A6** | 2 | 4 | 4 | 8 | 8 | 4 | 8 | 2 | 2 | 2 |
| **FLC** | 4 | 32 | >64 | 32 | >64 | 2 | 16 | 2 | 4 | 4 |

13

**Compounds A4 and A6 Showed Effective Inhibitory Activities against *C. neoformans*.** To further evaluate the antifungal profiles of compounds **A4** and **A6**, time-growth curves were prepared. Both compounds exhibited potent fungistatic activities. Compounds **A4** and **A6** inhibited *C. neoformans* H99 growth in a concentration-dependent manner and completely inhibited H99 cell growth at 8 μg/mL. In contrast, FLC did not obviously inhibit *C. neoformans* H99 growth in a concentration-dependent manner (**Figure 2**).
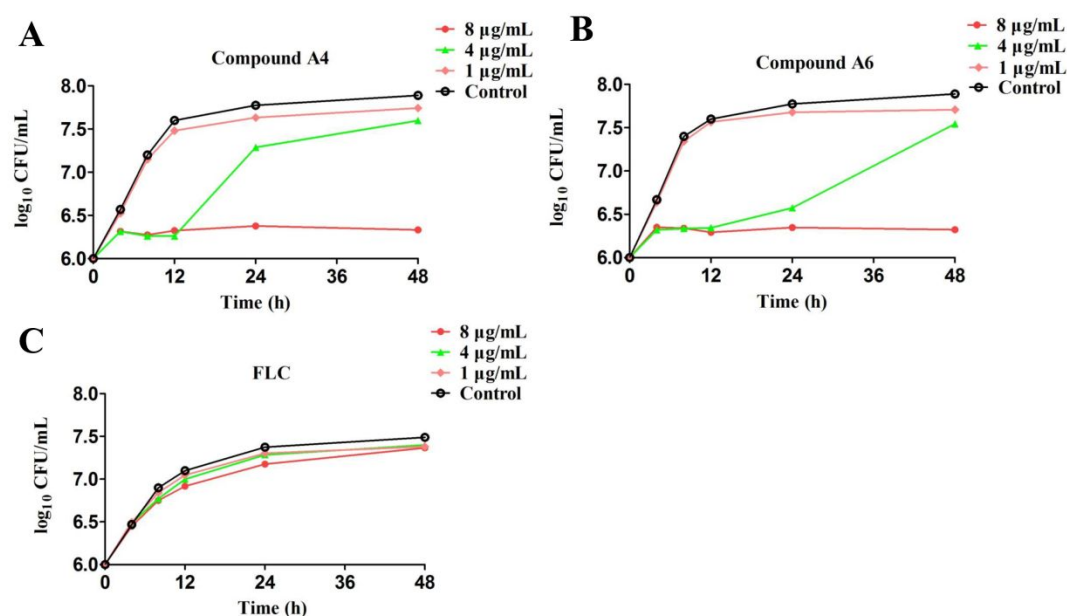


**Figure 2.** Fungal growth curves of *C. neoformans* H99 obtained by using initial inoculums containing $10^6$ colony-forming units (CFU)/mL. CFUs/mL were determined after 0, 4, 8, 12, 24 and 48 h of incubation. *C. neoformans* H99 was treated with different concentrations of compounds **A4** (**A**), **A6** (**B**) and FLC (**C**).

14

**Compounds A4 and A6 Inhibited the Formation of *C. neoformans* Biofilms.**

Fungal biofilm formation is closely related to drug resistance and repeated infection.[20] The adhesion of fungi to a surface is the first stage in this process.[20] Therefore, the effects of different concentrations of FLC and compounds **A4** and **A6** on the adherence of *C. neoformans* H99 cells (90 min) and subsequent biofilm formation were investigated using the XTT reduction assay.[21] Compounds **A4** and **A6** could significantly inhibit biofilm formation and were more active than FLC. At a concentration of 16 μg/mL, compounds **A4** and **A6** almost completely disrupted the formation of *C. neoformans* biofilms (**Figure 3**). The effects of FLC and compound **A4** on the cellular surface hydrophobicity (CSH) of *C. neoformans* H99 were also investigated. Compound **A4** significantly decreased the CSH of *C. neoformans* ($P < 0.001$, **Figure 4**), whereas FLC was ineffective.

15
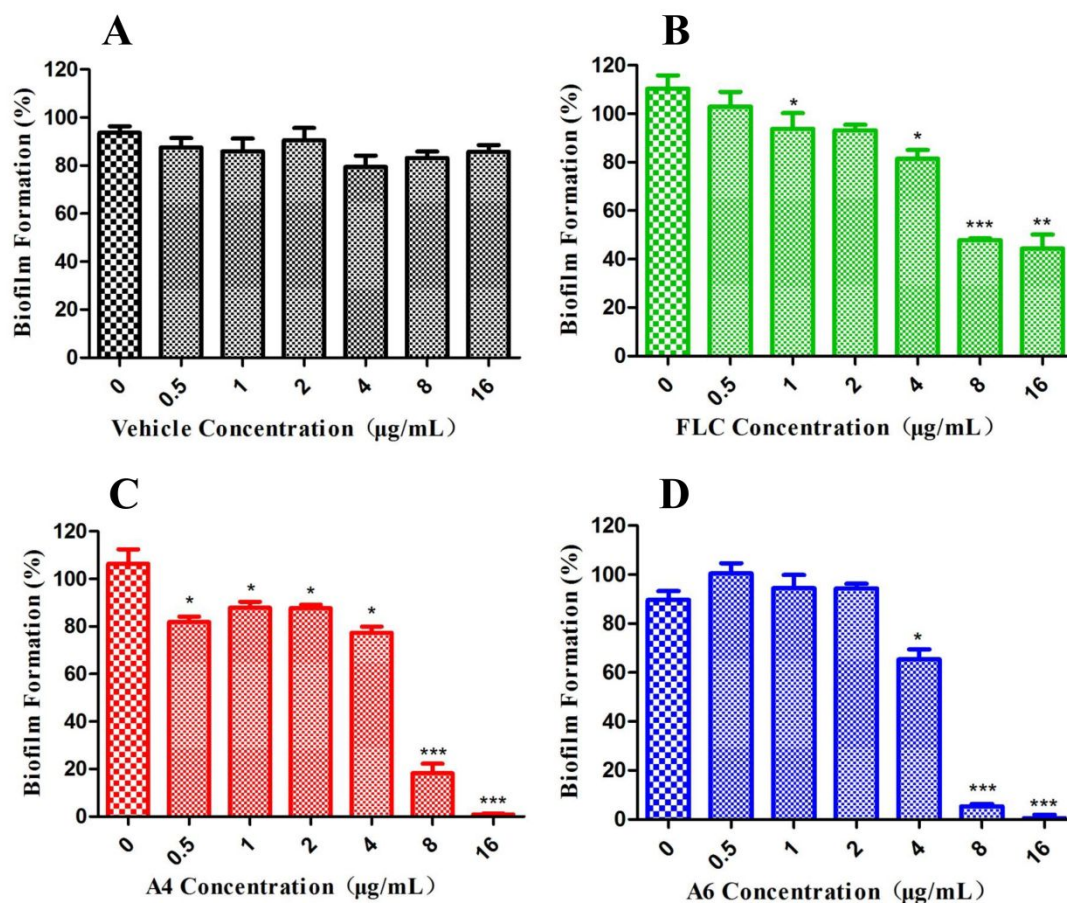
**Figure 3.** Effects of different concentrations of DMSO (**A**), FLC (**B**), compound **A4** (**C**) and compound **A6** (**D**) on the adherence of *C. neoformans* H99 cells (90 min) and subsequent biofilm formation using the XTT reduction assay. The values are the mean absorbance values (optical density (OD)) at 490 nm and standard deviations (SDs) of triplicate analyses. The results are presented as a percentage compared to the control group, which was untreated. * $P < 0.05$, ** $P < 0.01$, *** $P < 0.001$ versus the control group.
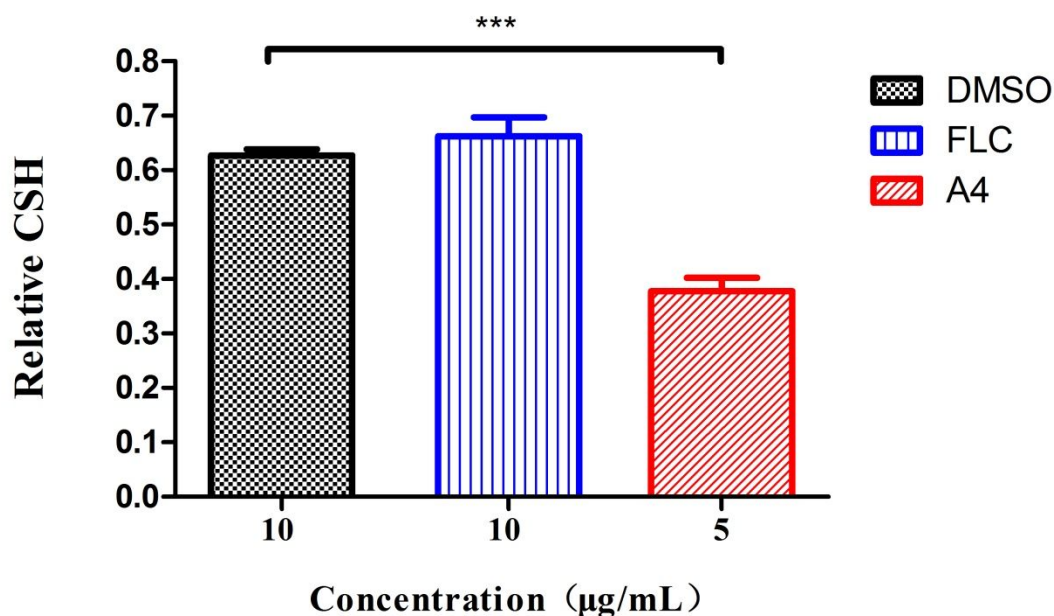
**Figure 4.** Effects of FLC and compound **A4** on the CSH of *C. neoformans* H99. Relative CSH values were obtained by a water-hydrocarbon two-phase assay. SDs are depicted and based on three independent experiments. *** $P < 0.001$.

**Compounds A4 and A6 Inhibited the Production of Melanin without Affecting that of Urease.** Melanin and urease are specific virulence factors of *C. neoformans* that play a significant role in pathogenic effects and immunity escape.[22, 23] In this study, specific inducing culture media were used to induce the production of melanin and urease.[24] The production of melanin and urease was identified by observing the features of the colonies and chromogenic reactions. *C. neoformans* H99 strains were treated with different concentrations of compounds **A4** and **A6** and then inoculated in the corresponding media. Compounds **A4** and **A6** at 2.5 μg/mL could inhibit the production of melanin, whereas FLC was inactive. However, **A4** and **A6** had no obvious inhibitory effects on the production of urease even at high concentrations

17
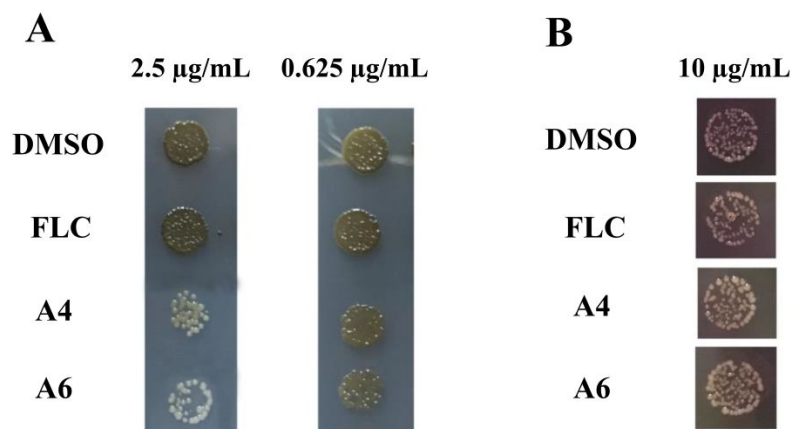
**Figure 5.** Effects of **A4**, **A6** and FLC on the production of melanin and urease in *C. neoformans* H99 cells. (**A**) Melanin production assay. Strains treated with different concentrations of the test compounds were grown on L-DOPA medium at 37°C. (**B**) Strains were grown on the urea medium at 37°C for the detection of urease production.

**Compound A4 Displayed Potent *in vivo* Antifungal Effects in a Murine Model of CM.** Before investigating their *in vivo* antifungal activities, their microsomal metabolic stabilities were tested. Compound **A4** had a low clearance rate in the liver microsomal metabolic stability test with a half-life ($T_{1/2}$) of 70 min, indicating that it may have good metabolic stability. In contrast, compound **A6** was unstable ($T_{1/2}$ = 11 min) in the mouse liver microsomal stability assay (**Table 5**). Furthermore, the permeability of the blood-brain barrier (BBB) to compound **A4** was tested by the parallel artificial membrane permeation assay (PAMPA). Compound **A4** could easily penetrate the BBB at a level comparable to that of caffeine (**Table 6**).[25]

18

**Table 5.** Metabolic stabilities of compounds **A4** and **A6** in mouse liver microsomes

| | $T_{1/2}$[a] (min) | $CL$[b] (mL/min/mg) |
|---|---|---|
| **Midazolam** | 2 | 2996 |
| **A4** | 70 | 78 |
| **A6** | 11 | 477 |

[a] Half-life. [b] Clearance.

**Table 6.** Permeability ($P_e \times 10^{-6}$ cm/s) and prediction of BBB penetration in the PAMPA-BBB assay for compound **A4**.

| | $P_e$[a] ($10^{-6}$ cm/s) | prediction [b] |
|---|---|---|
| **Caffeine** | $1.4 \pm 0.03$ | CNS± |
| **A4** | $1.8 \pm 0.14$ | CNS± |

[a] Values are expressed as the mean ± SD of at least three independent experiments.

[b] Compounds with $Pe > 3.08 \times 10^{-6}$ cm/s can cross the BBB by passive diffusion (CNS+). Compounds with $Pe < 1.13 \times 10^{-6}$ cm/s cannot cross the BBB (CNS−), and compounds with $1.13 \times 10^{-6}$ cm/s $< Pe < 3.08 \times 10^{-6}$ cm/s show uncertain BBB permeation (CNS±).

Considering the good metabolic stability and BBB penetration of compound **A4**, we evaluated its *in vivo* antifungal activity using a CM model. Mice CM models were established by injecting *C. neoformans* H99 cells into the tail veins of the animals. Mice were assigned into three groups: the control group, the FLC treatment group and

19

the **A4** treatment group. FLC and **A4** treatment were initiated at 24 h postinfection by

oral administration. The treatments were continued for 5 consecutive days. The mice

were sacrificed 5 days postinfection, and their brain fungal burdens were determined

by measuring the number of CFU. Treatment with compound **A4** significantly

reduced the fungal burden in the brain ($P < 0.001$), and it was more effective than

FLC ($P < 0.001$). (**Figure 6**). The brain fungal burden could also be significantly

reduced by intraperitoneal injection of **A4** at a dosage of 10 mg/kg once daily ($P <$

0.001, **Figure S2** in the Supporting Information). The results highlighted the potential

of compound **A4** for the treatment of CM.
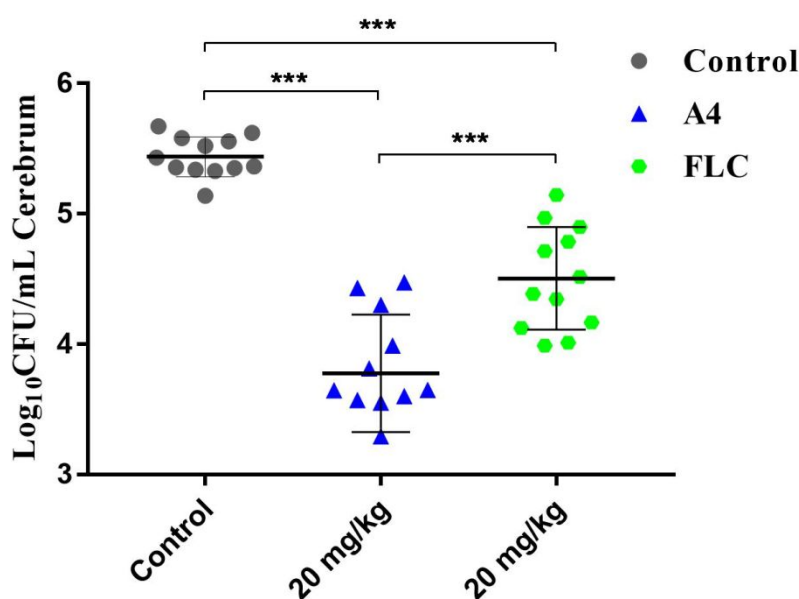


**Figure 6.** The therapeutic efficacies of compound **A4** and FLC in the *C. neoformans*

H99 CM model. Brain burdens of fungi (in $Log_{10}$ CFU/mL of brain) are shown for

mice treated with the indicated doses of **A4** or FLC for 5 days after infection with *C.*

*neoformans* H99. Data are presented as the mean ± SD. * $P < 0.05$, ** $P < 0.01$, ***

$P < 0.001$, determined by ANOVA.

1
2
3
4
5
6
7
8
9
10
11
12
13
14
15
16
17
18
19
20
21
22
23
24
25
26
27
28
29
30
31
32
33
34
35
36
37
38
39
40
41
42
43
44
45
46
47
48
49
50
51
52
53
54
55
56
57
58
59
60

**Cell Wall and Cell Membrane Collapse, Chromosome Condensation and Nuclear Pyknosis Effects of Compound A4 Contributed to the Inhibition *C. neoformans.*** To clarify the antifungal mechanism of compound **A4,** its influence on the morphology of *C. neoformans* was monitored by transmission electron microscopy (TEM). Normal *C. neoformans* cells and cells treated with FLC at 4 μg/mL for 24 h were used as controls. As shown in **Figure 7A**, normal *C. neoformans* cells have a uniform central density and a regular, well-outlined cell wall. The cells treated with FLC had damaged cell membranes and fragmented nuclei, but the cell walls were intact (**Figure 7B**). In contrast, after treatment with **A4** at 4 μg/mL for 24 h, the *C. neoformans* cells became abnormally shaped (**Figure 7C**). Cell wall collapse and nuclear pyknosis could also be observed (**Figure 7C**). Thus, **A4** and FLC may act by different antifungal mechanisms.
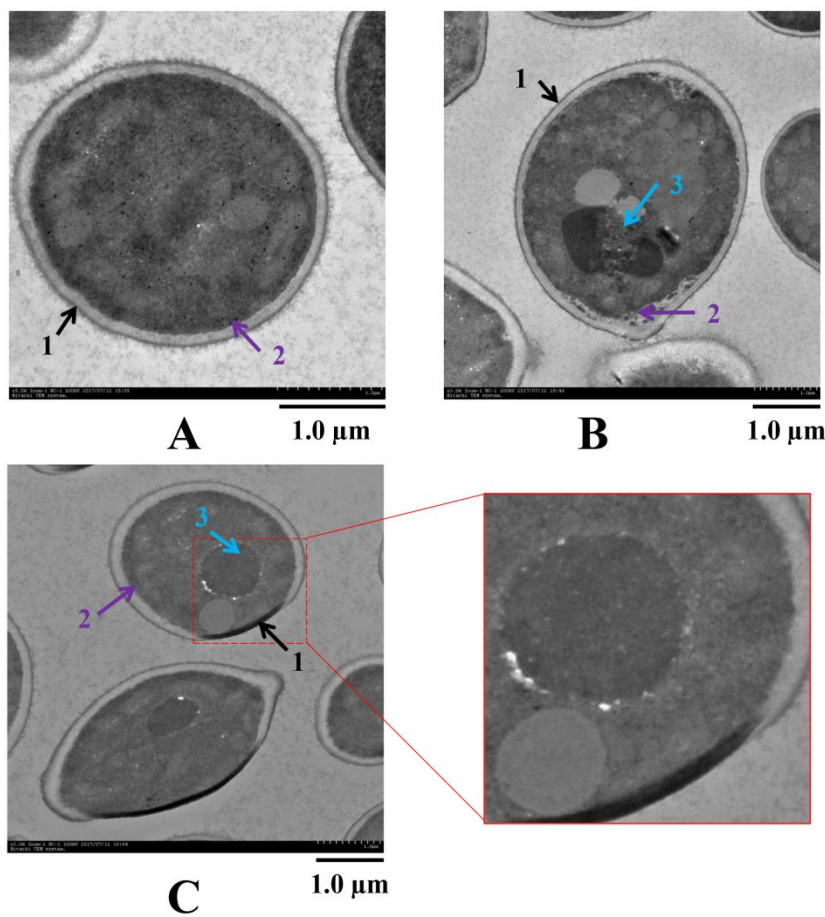
**Figure 7.** Transmission electron micrographs of *C. neoformans* H99 cells under different conditions. The arrows indicate organelles as follows: 1, cell wall; 2, cell membrane; 3, cell nucleus. (**A**) Normal *C. neoformans* cells; (**B**) fungal cells treated with FLC at 4 μg/mL for 24 h; and (**C**) fungal cells treated with compound **A4** at 4 μg/mL for 24 h.

**The Cdc25c/CDK1/Cyclin B Pathway is Essential for A4-Induced G2/M phase arrest.** Inspired by the morphological changes to *C. neoformans* cells treated with **A4** and FLC, the impacts of the two compounds on the cell cycle were further investigated using flow cytometric analysis. Interestingly, after 24 h of exposure, 51.64% of the cells were in S phase, 44.50% of the cells were in G1 phase and 3.86%

22

of the cells were in G2 phase in the control, compared to 48.17%, 50.86% and 0.96%, respectively, in the sample treated with 4 µg/mL FLC. The results indicated that FLC induced cell cycle arrest at the G1 phase. In contrast, compound **A4** arrested the G2/M phase of the cell cycle (53.21% in S phase, 36.45% in G1 phase and 10.34% in G2 phase, **Figure 8**). The Cdc25c/CDK1/cyclin B pathway is associated with G2/M phase control.[26] To further investigate the mode of action of **A4-**induced G2/M phase arrest, the expression levels of CDK1 and cyclin B were evaluated by Western blot. As shown in **Figure 9A** and **9B**, compound **A4** upregulated the expression of CDK1 and Cdc25c in a dose-dependent manner, whereas FLC did not obviously influence the expression of CDK1 and Cdc25c. The results revealed that compound **A4** induced cell cycle arrest at the G2 phase by acting on the Cdc25c/CDK1/cyclin B pathway.
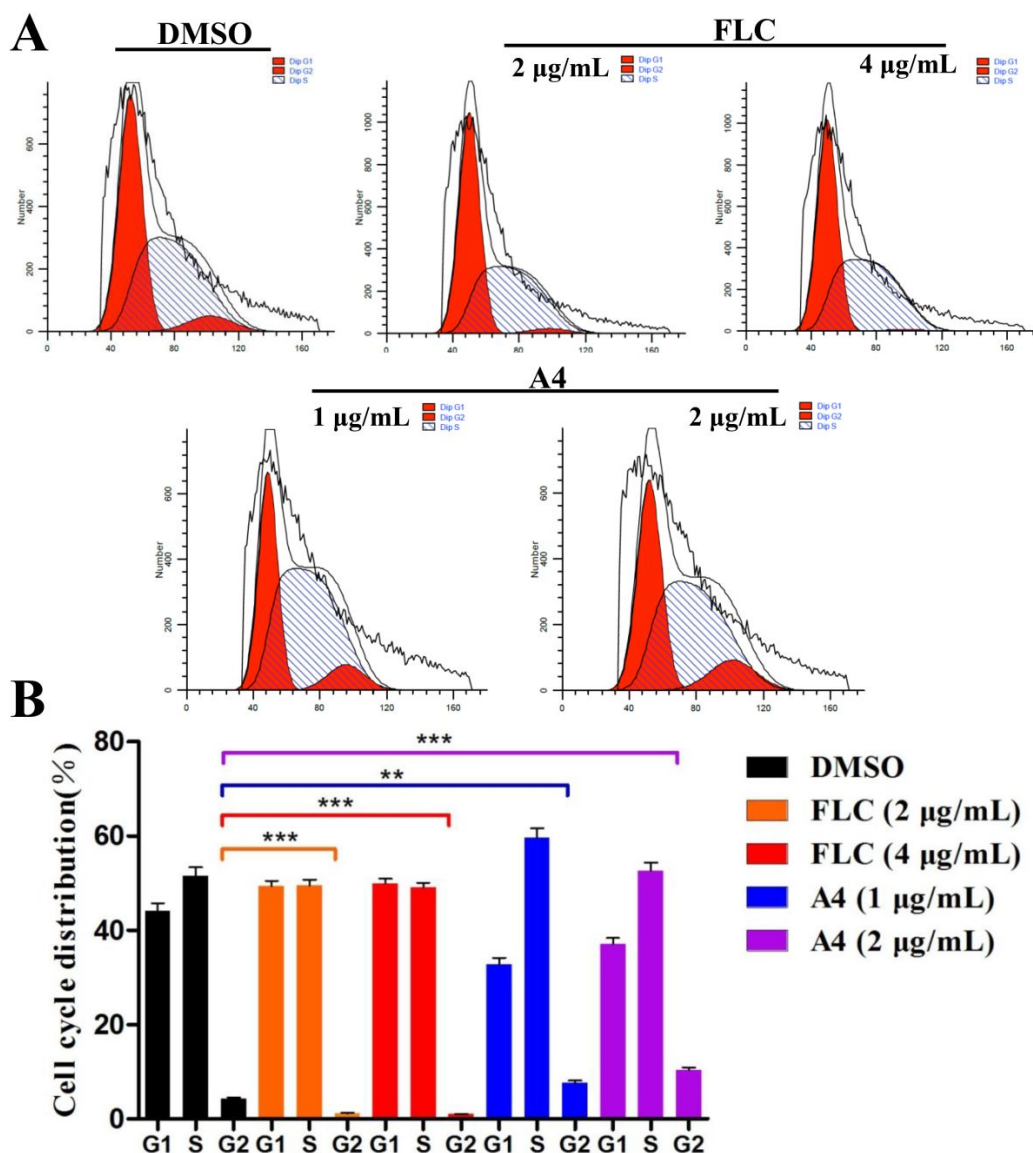
**Figure 8**. Flow cytometric analysis and cell cycle arrest by compound **A4**. (**A**) Cell cycle analysis by flow cytometry. *C. neoformans* H99 cells were treated with different concentrations of FLC and **A4** for 24 h after staining with PI. Determinations were performed in triplicate, and one representative experiment is shown. (**B**) Mean percentages of cells in $G_1$, S, and $G_2$ phases. The percentages in different phases were calculated by flow cytometry software. Data are presented as the mean ± SD from three independent experiments. ** $P < 0.01$, *** $P < 0.001$, determined by ANOVA.

24
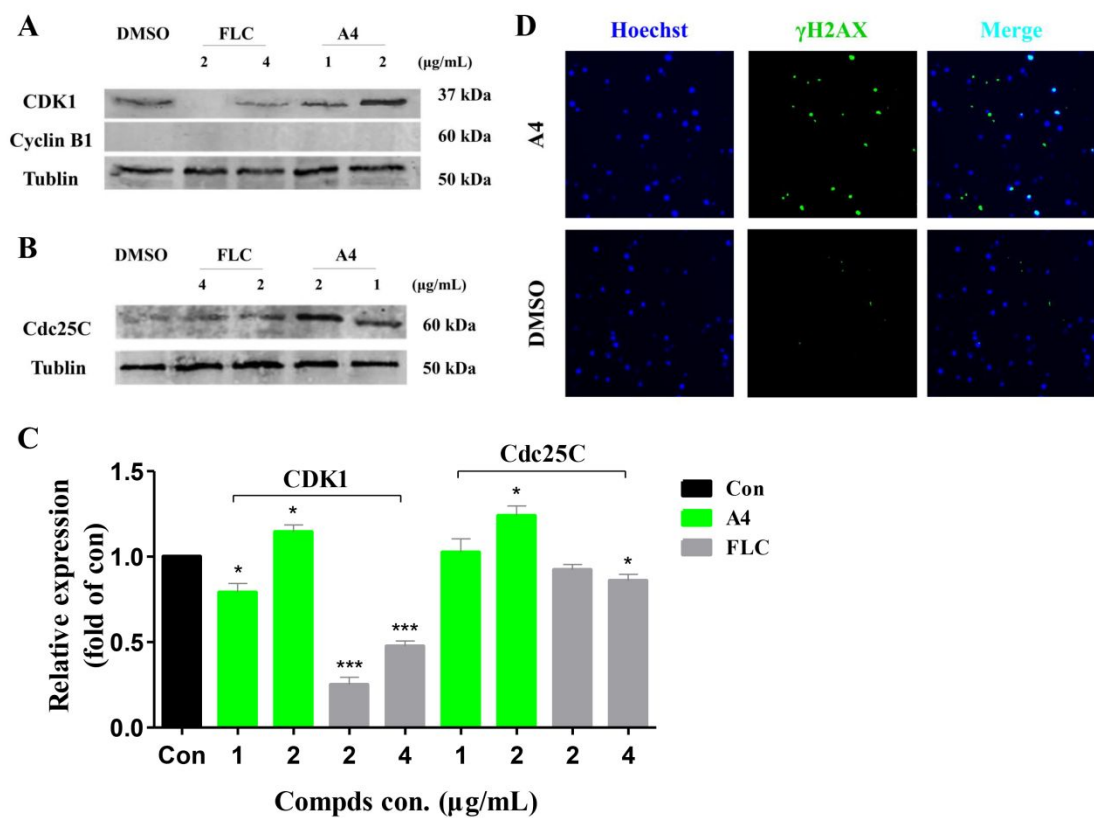
**Figure 9.** Effects of compounds **A4** and FLC on the expression levels of CDK1 (**A**), cyclin B1 (**A**) and Cdc25C (**B**) in *C. neoformans* H99 cells. (**C**) Gray intensity analysis of the Western blots. (**D**) *C. neoformans* H99 cells were treated with **A4** at 2 µg/mL for 48 h and assayed for DNA damage by immunofluorescence staining with Hoechst 33342 (blue) and γH2AX (green). * $P < 0.05$, ** $P < 0.01$, *** $P < 0.001$ versus the control group.

**Compound A4 Induces DNA Damage and Increases Nuclear *γ*-H2AX Foci.** In the presence of DNA double stranded breaks (DSBs), cells arrest in the G2/M phase to allow time to repair the damage.[27] In addition, histone H2AX is phosphorylated by ataxia telangiectasia mutated (ATM), termed γ-H2AX, which is a major cascade. Hence, γ-H2AX is a sensitive biomarker for DSBs.[28, 29] In this study, the effects of

25

treatment with **A4** on DSBs in *C. neoformans* H99 cells were investigated. As shown in **Figure 9C**, compound **A4** induced γH2AX expression, which was colocalized with Hoechst staining in *C. neoformans* H99. **A4** increased the appearance of nuclear γ-H2AX foci and induced DSBs.

**KEGG Pathways Analysis of DEGs was Consistent with the Induction of G2/M Phase Arrest and DSBs by A4.** To further understand the changes in biological processes upon treatment with compound **A4**, RNA-sequencing (poly A) analysis of *C. neoformans* H99 cells was performed. Kyoto encyclopedia of genes and genomes (KEGG) enrichment analysis was performed to classify the functions of the differentially expressed genes (DEGs, **Figures S3** and **S4** in the Supporting Information).[30-34] Notably, 12 DEGs were enriched in the cell cycle (cell cycle and the yeast cell cycle), and 6 DEGs were enriched related to DNA replication. In the cell cycle, the 12 upregulated DEGs included APC/C (CNAG_00320 and CNAG_02963), PNAC (CNAG_06079), PLK1 (CNAG_01907), MCM (CNAG_03341, CNAG_05825 and CNAG_06182), ORC (CNAG_06183), Mps1 (CNAG_06697), Hsl7 (CNAG_02829), Ycg1 (CNAG_00681) and Mob1 (CNAG_05541). In DNA replication, the 6 upregulated DEGs included Lig1 (CNAG_04278), DNA polymerase α2 (CNAG_06142), PCNA and MCM (**Figure 10, Table 7**). These genes are closely related to cell division, the regulation of mitotic metaphase/anaphase transitions and DNA replication.
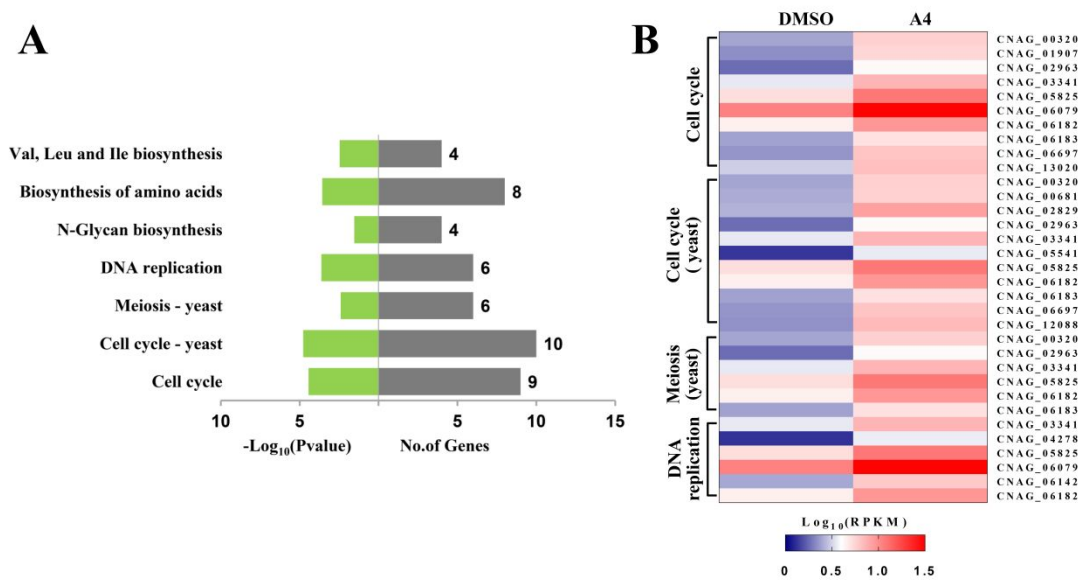
**Figure 10.** *C. neoformans* H99 cells were treated with compound **A4** at 2 μg/mL or DMSO for 24 h, and RNA–seq analysis was performed. (**A**) Significantly enriched pathway in terms of their differentially expressed genes based on KEGG analysis. (**B**) Heatmaps showing selected gene panels involved in pathways related to those described in (**A**); red, induced; blue, suppressed; $\log_{10}$(RPKM)-based scale.

**Table 7.** Signaling pathway enrichment analysis of differentially expressed genes.

| KEGG Pathway | Count | P-Value | Genes |
|---|---|---|---|
| Cell cycle | 9 | $3.6 \times 10^{-6}$ | CNAG_00320 CNAG_01907 CNAG_02963 CNAG_03341 CNAG_05825 CNAG_06079 CNAG_06182 CNAG_06183 CNAG_06697 |
| Cell cycle - yeast | 10 | $1.7 \times 10^{-6}$ | CNAG_00320 CNAG_00681 CNAG_02829 CNAG_02963 CNAG_03341 CNAG_05541 CNAG_05825 CNAG_06182 CNAG_06183 |

| | | | |
|---|---|---|---|
| | | | CNAG_06697 |
| Meiosis - yeast | 6 | $3.9 \times 10^{-3}$ | CNAG_00320 CNAG_02963 CNAG_03341 |
| | | | CNAG_05825 CNAG_06182 CNAG_06183 |
| DNA replication | 6 | $2.4 \times 10^{-4}$ | CNAG_03341 CNAG_04278 CNAG_05825 |
| | | | CNAG_06079 CNAG_06142 CNAG_06182 |
| N-Glycan biosynthesis | 4 | $2.9 \times 10^{-2}$ | CNAG_02855 CNAG_04364 CNAG_04743 |
| | | | CNAG_06901 |
| Biosynthesis of amino acids | 8 | $2.7 \times 10^{-4}$ | CNAG_00450 CNAG_02812 CNAG_05398 |
| | | | CNAG_05725 CNAG_05899 CNAG_06421 |
| | | | CNAG_06849 CNAG_07529 |
| Valine, leucine and isoleucine biosynthesis | 4 | $3.4 \times 10^{-3}$ | CNAG_00450 CNAG_05725 CNAG_06421 |
| | | | CNAG_07529 |

## CONCLUSION

The discovery of novel lead compounds for the treatment of CM remains a significant challenge. Herein, a series of new *β*-tetrahydrocarboline derivatives were shown to possess potent anticryptococcal activities. In particular, compound **A4** showed several advantages as a promising lead compound for the development of next-generation CM therapeutic agents. First, it showed potent *in vitro* and *in vivo* anticryptococcal activities with good metabolic stability and BBB permeability. Compound **A4** demonstrated potent fungistatic activity against *C. neoformans* and significantly reduced the brain fungal burdens in a murine model of CM following oral

28

administration. Second, compound **A4** inhibited several virulence factors of *C. neoformans,* such as biofilm formation and the production of melanin, whereas FLC was completely inactive. Finally, compound **A4** may act by a new mode of action. Preliminary mechanistic studies revealed that compound **A4** induced DSBs and cell cycle arrest at G2 phase by acting on the Cdc25c/CDK1/cyclin B pathway. Cell wall and cell membrane collapse, chromosome condensation and nuclear pyknosis were observed by TEM after treating *C. neoformans* cells with compound **A4**. Further structural optimization, mechanism and target verification studies are in progress.

**EXPERIMENTAL SECTION**

**Chemistry.** *General methods.* ^{1}H NMR and ^{13}C NMR spectra were recorded on Bruker AVANCE300, AVANCE500 or AVANCE600 spectrometers (Bruker Company, Germany) using TMS as an internal standard and CDCl$_3$ or DMSO-*d6* as solvents. Chemical shifts and coupling constants are given in ppm (*δ* values) and Hz (*J* values). Elemental analyses were performed with a MOD-1106 instrument and were consistent with theoretical values within 0.4%. The mass spectra were recorded on an Esquire 3000 LC-MS mass spectrometer. Silica gel thin-layer chromatography separations were performed on precoated plates GF-254 (Qingdao Haiyang Chemical, China). All solvents and reagents were analytically pure, and no further purification steps were needed. All starting materials were commercially available. The purities of the compounds were determined by HPLC (Agilent 1260) using MeOH as the mobile phase at a flow rate of 0.6 mL/min on a C18 column, and all final compounds exhibited purities greater than 98%.

Starting from the appropriate substituted tryptamines, intermediates **5a-q** were prepared according to previously reported methods.[19]

**1-(3-Bromopropoxy)-4-chlorobenzene (4a).** A solution of 1,3-dibromopropane (2.00 g, 9.9 mmol) was added dropwise to a mixture of tetrachlorophenol (0.64 g, 5.00 mmol) and $K_2CO_3$ (0.69 g, 5.00 mmol) in EtOH (10 mL). The mixture was stirred at 80°C for 4 h and then filtered. The filtrate was concentrated and then diluted with $H_2O$ (20 mL) and extracted with EtOAc (30 mL × 3). The organic layers were combined, dried with $Na_2SO_4$ and concentrated under reduced pressure. The residue was purified by column chromatography (CC) to give intermediate **4a** (0.80 g, 64%) as a transparent oil. ^{1}H NMR (600 MHz, $CDCl_3$) $\delta$: 7.26-7.25 (m, 1H), 7.25-7.24 (m, 1H), 6.85-6.84 (m, 1H), 6.84-6.83 (m, 1H), 4.08 (t, $J$ = 5.8 Hz, 2H), 3.60 (t, $J$ = 6.4 Hz, 2H), 3.56 (t, $J$ = 6.2 Hz, 2H). MS (ESI positive): m/z [M+H]$^+$: 249.12.

Compounds **A1-A30** were synthesized according to a protocol similar to that described for **A30**.

**6-Chloro-9-(3-(4-chlorophenoxy)propyl)-2,3,4,9-tetrahydro-1*H*-pyrido[3,4-*b*]indo le 2,2,2-trifluoroacetate (A4).** Brown solid, 0.30 g, yield 84.40%. ^{1}H NMR (600 MHz, DMSO-$d_6$) $\delta$: 9.43 (s, 2H), 7.58 (d, $J$ = 1.4 Hz, 1H), 7.51 (d, $J$ = 8.7 Hz, 1H), 7.33 (d, $J$ = 8.8 Hz, 2H), 7.13 (dd, $J$ = 8.7, 1.6 Hz, 1H), 6.95 (d, $J$ = 8.9 Hz, 2H), 4.46 (s, 2H), 4.28 (t, $J$ = 6.9 Hz, 2H), 3.91 (t, $J$ = 5.9 Hz, 2H), 3.43 (d, $J$ = 4.9 Hz, 2H), 2.93 (t, $J$ = 5.6 Hz, 2H), 2.09 (p, $J$ = 6.4 Hz, 2H).^{13}C NMR (151 MHz, $CD_3OD$) $\delta$: 157.17, 135.40, 129.02, 127.92, 127.06, 125.50, 125.25, 122.15, 117.40, 115.55, 110.62, 105.61, 64.14, 41.99, 39.99, 39.65, 29.03, 17.85. HRMS m/z calcd for $C_{20}H_{21}Cl_2N_2O$ [M+H]$^+$ 375.1025, found 375.1027. HPLC purity 99.8%. Retention time: 10.4 min, eluted with MeOH.

**6-Bromo-9-(3-(4-chlorophenoxy)propyl)-2,3,4,9-tetrahydro-1*H*-pyrido[3,4-*b*]indo**

le 2,2,2-trifluoroacetate (A5). Brown solid, 0.14 g, yield 82.35%. $^1$H NMR (600 MHz, DMSO-$d_6$) $\delta$: 9.28 (s, 2H), 7.71 (d, $J$ = 1.7 Hz, 1H), 7.47 (d, $J$ = 8.7 Hz, 1H), 7.32 (d, $J$ = 9.0 Hz, 2H), 7.23 (dd, $J$ = 8.7, 1.9 Hz, 1H), 6.94 (d, $J$ = 9.0 Hz, 2H), 4.44 (s, 2H), 4.26 (t, $J$ = 6.8 Hz, 2H), 3.90 (t, $J$ = 6.0 Hz, 2H), 3.42 (s, 2H), 2.92 (t, $J$ = 5.8 Hz, 2H), 2.14-2.03 (m, 2H). $^{13}$C NMR (151 MHz, CD$_3$OD) $\delta$: 157.17, 135.67, 129.02, 127.77, 127.69, 125.51, 124.79, 120.56, 115.55, 112.58, 111.05, 105.52, 64.14, 41.99, 39.97, 39.65, 29.01, 17.85. HRMS m/z calcd for $C_{20}H_{21}BrClN_2O$ [M+H]$^+$ 421.0500, found 421.0499.

**9-(3-(4-Chlorophenoxy)propyl)-6-methyl-2,3,4,9-tetrahydro-1$H$-pyrido[3,4-$b$]ind ole 2,2,2-trifluoroacetate (A6).** Brown solid, 0.15 g, yield 85.35%. $^1$H NMR (600 MHz, DMSO-$d_6$) $\delta$: 9.26 (s, 2H), 7.33 (t, $J$ = 8.9 Hz, 3H), 7.26 (s, 1H), 6.95 (d, $J$ = 8.8 Hz, 3H), 4.41 (s, 2H), 4.22 (t, $J$ = 6.9 Hz, 2H), 3.90 (t, $J$ = 6.0 Hz, 2H), 3.42 (d, $J$ = 5.4 Hz, 2H), 2.90 (t, $J$ = 5.7 Hz, 2H), 2.36 (s, 3H), 2.07 (p, $J$ = 6.2 Hz, 2H).$^{13}$C NMR (151 MHz, CD$_3$OD) $\delta$: 157.23, 135.39, 129.01, 128.75, 126.28, 126.03, 125.43, 123.63, 117.55, 115.56, 108.97, 105.22, 64.17, 42.16, 40.14, 39.36, 29.11, 20.01, 18.03. HRMS m/z calcd for $C_{21}H_{24}ClN_2O$ [M+H]$^+$ 355.1572, found 355.1573. HPLC purity 99.1%. Retention time: 14.1 min, eluted with MeOH.

**9-(3-(4-Chlorophenoxy)propyl)-6-methoxy-2,3,4,9-tetrahydro-1$H$-pyrido[3,4-$b$]in dole 2,2,2-trifluoroacetate (A7).** Brown solid, 0.13 g, yield 70.96%. $^1$H NMR (600 MHz, DMSO-$d_6$) $\delta$: 9.57 (s, 2H), 7.35 (d, $J$ = 8.9 Hz, 1H), 7.34-7.30 (m, 2H), 6.98 (d, $J$ = 2.3 Hz, 1H), 6.97-6.92 (m, 2H), 6.75 (dd, $J$ = 8.9, 2.4 Hz, 1H), 4.41 (s, 2H), 4.21 (t, $J$ = 6.9 Hz, 2H), 3.89 (t, $J$ = 6.0 Hz, 2H), 3.75 (s, 3H), 3.42 (d, $J$ = 5.8 Hz, 2H), 2.90 (t, $J$ = 5.8 Hz, 2H), 2.07 (p, $J$ = 6.4 Hz, 2H). $^{13}$C NMR (151 MHz, CD$_3$OD) $\delta$: 158.56, 157.10, 153.82, 137.41, 129.30, 125.47, 124.70, 123.18, 118.57, 116.52,

114.70, 112.62, 105.66, 102.91, 99.85, 82.39, 65.08, 55.29, 42.08, 29.48, 20.04.

HRMS m/z calcd for $C_{21}H_{24}ClN_2O_2$ [M+H]$^+$ 371.1521, found 371.1531.

**9-(3-(4-Chlorophenoxy)propyl)-2,3,4,9-tetrahydro-1*H*-pyrido[3,4-*b*]indole 2,2,2-trifluoroacetate (A30).** NaH (0.03 g, 1.23 mmol) was added in portions over 5 min to a stirred solution of intermediate **5q** (0.11 g, 0.41 mmol) in DMF (10 mL) in an ice bath. The mixture was stirred at room temperature for 0.5 h. Then, intermediate **4a** (0.15 g, 0.61 mmol) was added, and the reaction was stirred at room temperature for 1 h. The mixture was diluted with water (10 mL) and extracted with EtOAc (10 mL × 3). The organic layers were combined, dried with $Na_2SO_4$, filtered and concentrated under reduced pressure. The residue was purified by column chromatography (hexane:EtOAc = 12: 1, v/v) to give intermediate **6** (0.16 g, 87.07%) as a pale-yellow solid. To a stirred solution of intermediate **6** (0.16 g, 0.36 mmol) in $CH_2Cl_2$ (4 mL), TFA (2 mL) was added dropwise in an ice bath. The mixture was stirred at room temperature for 0.5 h and then concentrated under reduced pressure to remove the $CH_2Cl_2$ and TFA. The residue was purified by column chromatography ($CH_2Cl_2$:MeOH = 100: 5, v/v) to afford target compound **A30** (0.12 g, 50.16%) as a brown solid. $^1$H NMR (600 MHz, CDCl$_3$) $\delta$: 9.59 (s, 2H), 7.50 (d, $J$ = 7.8 Hz, 1H), 7.34 (d, $J$ = 8.2 Hz, 1H), 7.23 (m, 3H), 7.16 (t, $J$ = 7.2 Hz, 1H), 6.79 (m, 2H), 4.43 (s, 2H), 4.23 (t, $J$ = 6.6 Hz, 2H), 3.81 (t, $J$ = 5.5 Hz, 2H), 3.47 (d, $J$ = 5.6 Hz, 2H), 3.08 (t, $J$ = 5.7 Hz, 2H), 2.28–2.07 (m, 2H). $^{13}$C NMR (151 MHz, CDCl$_3$) $\delta$: 161.81, 161.56, 156.81, 136.90, 129.51, 126.14, 126.00, 125.45, 122.88, 120.12, 118.58, 115.69, 109.50, 106.30, 64.10, 42.63, 40.47, 39.96, 29.36, 18.58. HRMS m/z calcd for $C_{20}H_{22}ClN_2O$ [M+H]$^+$ 341.1415, found 341.1420.

***tert*-Butyl-9-(3-bromopropyl)-3,4-dihydro-1*H*-pyrido[3,4-*b*]indole-2(9*H*)-carboxylate (7).** NaH (0.067 g, 2.76 mmol) was added in portions to a stirred solution of

intermediate **5q** (0.50 g, 1.84 mmol) in DMF (10 mL) in an ice bath. Then, 1,3-dibromopropane was added dropwise, and the mixture was stirred at room temperature for 1 h. The resulting mixture was quenched with water (20 mL) and extracted with EtOAc (20 mL × 3). The organic layers were combined, dried with $Na_2SO_4$, filtered and concentrated under reduced pressure. The residue was purified by column chromatography using hexane:EtOAc (8: 1, v/v) to give intermediate **7** (0.34 g, 47.07%) as a pale-yellow solid. ^{1}H NMR (300 MHz, $CDCl_3$) $\delta$: 7.52 (d, $J$ = 7.6 Hz, 1H), 7.38 (d, $J$ = 8.0 Hz, 1H), 7.23 (t, $J$ = 7.4 Hz, 1H), 7.14 (t, $J$ = 7.3 Hz, 1H), 4.70 (s, 2H), 4.21 (t, $J$ = 6.7 Hz, 2H), 3.79 (s, 2H), 3.40 (t, $J$ = 6.1 Hz, 2H), 2.84 (s, 2H), 2.43-2.26 (m, 2H), 1.55 (s, 9H). MS (ESI positive): m/z [M+H]$^+$: 395.43.

**4-Chloro-*N*-(3-(3,4-dihydro-1*H*-pyrido[3,4-*b*]indol-9(2*H*)-yl)propyl)aniline 2,2,2-trifluoroacetate (B1).** Intermediate **7** (0.10 g, 0.25 mmol), parachloroaniline (0.065 g, 0.51 mmol) and $K_2CO_3$ (0.035 g, 0.25 mmol) were added to MeCN (5 mL), and the mixture was stirred at 85°C for 1 h. Then, the resulting mixture was concentrated, and the residue was purified by column chromatography (hexane:EtOAc = 20: 1, v/v) to give intermediate **8** (0.94 g, 85.32%) as a pale-yellow solid. TFA (2 mL) was added dropwise to a stirred solution of intermediate **8** (0.94 g, 0.21 mmol) in $CH_2Cl_2$ (4 mL) in an ice bath. Then, the mixture was stirred at room temperature for 0.5 h and concentrated under the reduced pressure to remove the $CH_2Cl_2$ and TFA. The residue was purified by column chromatography ($CH_2Cl_2$:MeOH = 100: 3, v/v) to afford target compound **B1** (0.52 g, 70.86%) as a yellow solid. ^{1}H NMR (600 MHz, DMSO-$d_6$) $\delta$: 9.34 (s, 2H), 7.52 (d, $J$ = 8.5 Hz, 2H), 7.17 (dd, $J$ = 13.9, 5.5 Hz, 1H), 7.14-7.10 (m, 2H), 7.08 (t, $J$ = 7.7 Hz, 1H), 6.62-6.57 (m, 2H), 4.45 (s, 2H), 4.23 (t, $J$

= 7.2 Hz, 2H), 3.52-3.42 (m, 2H), 2.98 (dt, $J$ = 11.9, 6.4 Hz, 2H), 1.95 (p, $J$ = 6.9 Hz, 2H). $^{13}$C NMR (151 MHz, CD$_3$OD) $\delta$: 147.47, 136.71, 135.09, 130.09, 126.14, 125.77, 120.06, 119.09, 118.67, 113.96, 112.54, 109.37, 106.45, 42.26, 41.92, 40.95, 40.39, 29.70, 18.52. HRMS m/z calcd for C$_{20}$H$_{23}$ClN$_3$ [M+H]$^+$ 340.1575, found 340.1587. HPLC purity 98.8%. Retention time: 11.7 min, eluted with MeOH.

Compounds **B2-B16** were synthesized according to a protocol similar to that described for **B1**.

**_N_-(3-(3,4-dihydro-1_H_-pyrido[3,4-_b_]indol-9(2_H_)-yl)propyl)-2-methoxyaniline 2,2,2 -trifluoroacetate (B4).** Light-yellow solid, 0.034 g, yield 57.63%. $^1$H NMR (600 MHz, DMSO-$d_6$) $\delta$: 9.35 (s, 2H), 7.48 (dd, $J$ = 15.3, 8.0 Hz, 2H), 7.15 (dd, $J$ = 11.2, 4.1 Hz, 1H), 7.06 (t, $J$ = 7.4 Hz, 1H), 6.81 (dd, $J$ = 7.9, 1.1 Hz, 1H), 6.74 (td, $J$ = 7.6, 1.3 Hz, 1H), 6.58 (d, $J$ = 7.5 Hz, 1H), 6.48 (d, $J$ = 8.0 Hz, 1H), 4.43 (s, 2H), 4.19 (t, $J$ = 7.1 Hz, 2H), 3.44 (d, $J$ = 5.9 Hz, 3H), 3.04 (t, $J$ = 7.0 Hz, 2H), 2.95 (t, $J$ = 6.0 Hz, 2H), 2.02-1.94 (m, 2H). $^{13}$C NMR (151 MHz, CD$_3$OD) $\delta$: 158.59, 147.18, 138.07, 136.78, 128.02, 126.17, 122.21, 121.53, 119.69, 118.62, 116.67, 116.30, 110.41, 110.21, 105.89, 55.82, 41.90, 41.21, 40.83, 29.59, 18.60. HRMS m/z calcd for C$_{21}$H$_{26}$N$_3$O [M+H]$^+$ 336.2070, found 336.2077.

**_N_-(3-(3,4-dihydro-1_H_-pyrido[3,4-_b_]indol-9(2_H_)-yl)propyl)-2-ethoxyaniline 2,2,2- trifluoroacetate (B5).** Light-yellow solid, 0.15 g, yield 88.76%. $^1$H NMR (600 MHz, DMSO-$d_6$) $\delta$: 9.38 (s, 2H), 7.46 (dd, $J$ = 18.2, 8.1 Hz, 2H), 7.13 (t, $J$ = 7.2 Hz, 1H), 7.04 (t, $J$ = 7.2 Hz, 1H), 6.79 (d, $J$ = 7.7 Hz, 1H), 6.71 (d, $J$ = 7.6 Hz, 1H), 6.54 (t, $J$ = 7.4 Hz, 1H), 6.49 (d, $J$ = 7.5 Hz, 1H), 4.42 (s, 2H), 4.17 (t, $J$ = 7.1 Hz, 2H), 3.99 (q, $J$

34

= 6.9 Hz, 2H), 3.43 (d, *J* = 4.7 Hz, 2H), 3.04 (t, *J* = 6.9 Hz, 2H), 2.93 (t, *J* = 5.7 Hz,

2H), 1.99-1.90 (m, 3H). $^{13}$C NMR (151 MHz, CD$_3$OD) *δ*: 146.73, 136.77, 128.00,

126.19, 122.18, 121.51, 119.68, 118.62, 117.83, 111.77, 111.46, 110.11, 105.98,

64.02, 49.05, 41.83, 41.27, 41.06, 29.44, 18.55, 15.15. HRMS m/z calcd for

C$_{22}$H$_{28}$N$_3$O [M+H]$^+$ 350.2227, found 350.2242.

***tert*-Butyl-9-(3-(piperidin-1-yl)propyl)-3,4-dihydro-1*H*-pyrido[3,4-*b*]indole-2(9*H*)**

**-carboxylate (9a).** Intermediate **7** (0.091 g, 0.23 mmol) and piperidine (0.059 g, 0.69

mmol) were added into DMF (5 mL), and the mixture was stirred at room temperature

for 2 h. The resulting mixture was quenched with water (20 mL) and extracted with

EtOAc (20 mL × 3). The organic layers were combined, dried with Na$_2$SO$_4$, filtered

and concentrated under reduced pressure. The residue was purified by column

chromatography (CH$_2$Cl$_2$:MeOH = 100: 4, v/v) to give intermediate **9a** (0.087 g,

94.56%) as a light-yellow solid. $^1$H NMR (300 MHz, CDCl$_3$) *δ*: 7.50 (d, *J* = 7.6 Hz,

1H), 7.36 (d, *J* = 8.0 Hz, 1H), 7.19 (t, *J* = 7.2 Hz, 1H), 7.11 (t, *J* = 7.3 Hz, 1H), 4.66

(s, 2H), 4.11 (t, *J* = 6.9 Hz, 2H), 3.77 (s, 2H), 2.82 (s, 2H), 2.52-2.34 (m, 6H), 2.06 (d,

*J* = 2.6 Hz, 2H), 1.69 (s, 6H), 1.53 (s, 9H). MS (ESI positive): m/z [M+H]$^+$: 398.56.

Intermediates **9b-l** were synthesized according to a protocol similar to that

described for **9a**. Compound **C1** was prepared from intermediate **9a** via deprotection

using a method similar to that of compound **B1**, but the CFA salts could not be

formed. The chemical synthesis of intermediate **11** was similar to that of intermediate

**7.** Compounds **C2-C14** were synthesized according to a protocol similar to that

described for **C1**.

**9-(3-(Piperidin-1-yl)propyl)-2,3,4,9-tetrahydro-1*H*-pyrido[3,4-*b*]indole       (C1).**

Light-yellow solid, 0.035 g, yield 53.50%. $^1$H NMR (600 MHz, DMSO-*d*$_6$) *δ*: 7.46 (t,

$J$ = 7.6 Hz, 2H), 7.14 (t, $J$ = 7.6 Hz, 1H), 7.03 (t, $J$ = 7.7 Hz, 1H), 4.36 (s, 2H), 4.11 (t,

$J$ = 6.9 Hz, 2H), 2.88 (t, $J$ = 5.8 Hz, 2H), 2.46 (s, 2H), 2.39-2.32 (m, 2H), 1.87 (d, $J$ =

6.7 Hz, 2H), 1.60-1.54 (m, 4H), 1.41 (s, 2H), 1.23 (s, 2H), 1.15 (t, $J$ = 7.3 Hz, 2H).

$^{13}$C NMR (151 MHz, CD$_3$OD) $\delta$: 136.51, 128.05, 126.58, 122.33, 119.83, 118.56,

109.15, 107.10, 54.51, 53.51, 42.24, 40.78, 31.92, 29.70. 24.98. 23.16. 22.69. 22.28.

19.27. HRMS m/z calcd for $C_{19}H_{28}N_3$ [M+H]$^+$ 298.2278, found 298.2286. HPLC

purity 98.7%. Retention time: 15.7 min, eluted with MeOH.

**Strains, culture and reagents.** Strains were routinely incubated in YPD (1% yeast

extract, 2% peptone and 2% dextrose) at 30°C in a shaking incubator. *C. neoformans*

H99 strains were provided by Changzheng Hospital of Shanghai, China. Stock

solutions of all compounds were prepared in DMSO at 2 mg/mL.

**Growth Curve Assay.** A growth curve assay was performed according to the

reported protocol[35] with a few modifications. Briefly, exponentially growing *C.*

*neoformans* H99 cells were harvested and resuspended in fresh RPMI 1640 medium

to a concentration of $1 \times 10^6$ cells/mL. Various concentrations of **A4**, **A6** and FLC

were added. The cells were cultured at 30°C with constant shaking (200 r.p.m.) and

counted at designated time points after culture (0, 4, 8, 12, 24 and 48 h). Neither FLC

nor the selected compounds were added to the control group. Three independent

experiments were performed.

***In vitro* Biofilm Formation Assay**. A biofilm formation assay was performed in a

96-well tissue culture plate (Corning, cat. no. 3599) by seeding with 100 μL of cell

suspensions ($1 \times 10^6$ cells/mL) in RPMI 1640 medium and statically incubating the

samples at 37°C. After 90 min of adhesion, the medium was aspirated, nonadherent

cells were removed, and different concentrations of **A4**, **A6** and FLC were added. The

plates were further incubated at 37°C for 24 h. A semiquantitative measure of the

formed biofilms was calculated using the XTT reduction assay.

**Antifungal susceptibility testing.** The test was performed as described previously

with a few modifications.[36] The initial concentration of the fungal suspension in

RPMI 1640 was $2 \times 10^3$ CFU/mL. Different concentrations of the test compounds

were added into the fungal suspension in 96-well plates, and the samples were

incubated at 35°C. The optical density of each well at 600 nm was detected by a

spectrophotometer and used to determine the inhibition of the growth of *C.*

*neoformans* H99. The $MIC_{80}$ value is the lowest concentration of the compound that

inhibited growth by 80% compared with the cell growth in the drug-free wells. Each

compound was tested in triplicate.

**Cellular surface hydrophobicity assay.** *C. neoformans* H99 CSH was measured as

described previously with a few modifications.[37, 38] Briefly, *C. neoformans* H99

biofilms were treated with the test compounds for 24 h and then removed from the

surface of the plate to prepare cell suspensions in PBS ($OD_{600} = 1.0$). Then, 1.2 mL of

suspension and 0.3 mL of octane were mixed by vortexing for 3 min. The mixture

was allowed to stand at room temperature for 3 min for phase separation, and then the

$OD_{600}$ of the aqueous phase was determined. The $OD_{600}$ of the group without the

octane overlay was used as the control. Three replicates were performed for each

group. Relative hydrophobicity was determined as [($OD_{600}$ of control - $OD_{600}$ after

octane overlay)/ $OD_{600}$ of the control] $\times$ 100%.

***In vitro blood−brain barrier permeation assay.*** Brain penetration by the test compounds was determined using PAMPA according to a previously reported protocol.[39] The acceptor 96-well microplate was filled with 300 μL of PBS:EtOH (7:3), and the filter membrane was impregnated with 4 μL of porcine brain lipid (PBL) in dodecane (20 mg/mL). The test compounds were dissolved in DMSO at 5 mg/mL and diluted to 100 μg/mL with PBS:EtOH (7:3). Then, 200 μL of this solution was added to the donor wells (PVDF membrane, pore size 0.45 mm). The acceptor filter plate was carefully placed on the donor plate to form a sandwich, and this stack was left undisturbed for 12 h at 25°C. After incubation, the donor plate was carefully removed, and the concentration of compounds in the acceptor wells was determined using a UV plate reader (SpectraMax i3). Three replicates were performed for each group.

***In vivo* Antifungal Potency.** Female ICR mice (4 to 6 weeks old and weighing 20 to 25 g) were housed and fed. After acclimatization for 1 week, the mice were infected through the tail vein with 0.2 mL of yeast suspension, which corresponded to $2 \times 10^5$ CFU of *C. neoformans* H99 in normal saline (NS) per mouse. Beginning 24 h after inoculation and continuing daily until the 6th day, FLC (20 mg/kg in NS) and compound **A4** (20 mg/kg suspended in NS with 1.5% glycerinum and 0.5% Tween 80) were administered orally. The control group consisted of mice treated with NS. On day 7, all mice were euthanized, after which their brains were removed and homogenized in NS (1 mL). Serial dilutions of the homogenates were inoculated on

38

SDA plates containing chloromycetin (100 μg/mL). The number of CFU/mL of the brain tissue was calculated and transformed into $Log_{10}$ units, and the differences between groups were analyzed by analysis of variance (ANOVA).

**Transmission Electron Microscopy.** Transmission electron microscopy images of *C. neoformans* H99 cells were obtained according to the reported protocol[40, 41] with a few modifications. Briefly, *C. neoformans* H99 cells were collected after 24 h of growth in liquid RPMI 1640 medium in the absence or presence of FLC (4 μg/mL) or compound **A4** (4 μg/mL) from an initial inoculum of $2 \times 10^6$ cells/mL. The cells were washed twice with PBS solution and fixed at 4°C for 24 h in 500 mL of fixative solution (sodium cacodylate buffer, pH 7.2, containing 4% polyoxymethylene). The samples were then washed with saline and postfixed for 90 min in 1% phosphotungstic acid. The fixed cells were dehydrated using a series of graded ethanol solutions and embedded in EPON-812. Ultrathin sections were prepared and observed under a transmission electron microscope (HITACHI H-800, Japan) with $1 \times 10^4$ magnification after double staining with uranium and lead.

**Cell cycle analysis by flow cytometry.** Cell cycle analysis was performed according to a previous protocol.[40] Exponentially growing *C. neoformans* H99 cells were harvested, washed twice with PBS, and resuspended in RPMI 1640 medium at $2 \times 10^6$ cells/mL. The cells were treated with different concentrations of compound **A4** and FLC. After incubation at 30°C with constant shaking (200 r.p.m.) for 24 h, 10 mL of each sample was centrifuged, washed, and fixed with 70% ethanol overnight. The cells were then stained with 50 μg/mL propidium iodide at 4°C for 30 min. The

samples were sonicated to separate the cells. Data were collected using a FACSCalibur cytometer (Becton, Dickinson, San Jose, CA) and analyzed with Cell Quest 3.0 software.

**Western Blotting.** Exponentially growing *C. neoformans* H99 cells were harvested, washed twice with PBS, and resuspended in RPMI 1640 medium at $2 \times 10^6$ cells/mL. Cells were exposed to compounds **A4** or FLC at 1, 2 and 4 µg/mL for 24 h and then harvested and washed twice with PBS. Then, the cells were lysed with RIPA cell lysis buffer on ice, glass beads (acid-washed, #G8772, SIGMA) were added, and the mixture was agitated (6500 r.p.m.) twice for 30 s each time. The cell lysates were centrifuged at $12000 \times g$ for 15 min at 4 °C. The supernatants were collected, and the BCA protein assay was used to determine the protein concentration. Equal amounts of protein (30 µg) were separated by SDS-PAGE. Then, the proteins were transferred to polyvinylidene fluoride membranes and blocked with 5% BSA for 2 h. The membranes were incubated with the primary antibody overnight at 4°C and washed with TBST three times. Then, the mixtures were incubated with the secondary antibody for 3 h. The membranes were washed with TBST three times. The immunoblots were visualized by Odyssey Infrared Imaging. The antibodies, including anti-CDK1 (#ab18, Abcam), anti-Cyclin B1 (#ab2949, Abcam), and anti-Cdc25C (#ab32444, Abcam), were purchased from Abcam.

**Melanin and urease production assays.** Exponentially growing *C. neoformans* H99 cells were harvested, washed twice with PBS, and resuspended in RPMI 1640 medium at $2 \times 10^6$ cells/mL. The cells were treated with different concentrations of

40

**A4**, **A6** and FLC and grown on L-DOPA or urea medium at 37°C to detect melanin and urease production.

**Immunofluorescent staining.** Exponentially growing *C. neoformans* H99 cells were harvested, washed twice with PBS, and resuspended in RPMI 1640 medium at $2 \times 10^6$ cells/mL. Culture medium containing DMSO or compound **A4** (2 μg/mL) was added. After incubation at 30°C with constant shaking (200 r.p.m.) for 24 h, 10 mL of each sample was centrifuged, washed, and fixed with 4% paraformaldehyde (PFA) in PBS overnight. After permeabilization with 10% methanol containing 0.1% Triton X-100 in PBS for 10 min, the cells were blocked with 5% normal donkey serum (#ab7475, Abcam) for 1 h. The cells were immunostained with anti-gamma H2AX (Phospho S139, #ab2893, Abcam) for 4 h and then stained with rabbit secondary antibody for 1 h. The nuclei were stained with Hoechst 33342 (0.5 μg/mL, #ab145597, Abcam) for 10 min. Fluorescence images were acquired with a fluorescence microscope (TCS-SP5).

**KEGG pathway enrichment analysis.** *C. neoformans* H99 cells were resuspended in RPMI 1640 medium at $2 \times 10^6$ cells/mL, treated with compound **A4** at 2 μg/mL or DMSO for 24 h. RNA–seq analysis was performed with illumine Hiseq 3000 (Ribobio Co. Ltd., China). The effects of compound **A4** on pathway enrichment were analyzed using online databases, and pathway analysis was carried out using the KEGG PATHWAY database (Available online: http://www.genome.jp/kegg)

■ **ASSOCIATED CONTENT**

**Supporting Information**

41

Antifungal spectrum, plasma protein binding and inhibition of normal human cells of compounds **A4** and **A6**. KEGG and DEG analyses of compound **A4**. Characterization data for the target compounds. $^1$H NMR spectra, HRMS data and HPLC chromatograms of the representative compounds, and Molecular Formula Strings of the target compounds.

The Supporting Information is available free of charge on the ACS Publications website at DOI: XXXXXX/acs.jmedchem.XXXXXXX.

■ **AUTHOR INFORMATION**

**Corresponding Author**

* (C. S.) Phone / Fax: +86 21 81871205. E-mail: shengcq@smmu.edu.cn

* (N. L.) Phone / Fax: +86 21 81871230. E-mail: liuna66@aliyun.com

**Author Contributions**

$^†$ Jie Tu and Zhuang Li contributed equally to this work.

The manuscript was written through contributions of all authors. All authors have given approval to the final version of the manuscript.

**Notes**

The authors declare no competing financial interest.

■ **ACKNOWLEDGMENT**

■ **ABBREVIATIONS LIST**

IFI, invasive fungal infection; CM, cryptococcal meningitis; EFA, early fungicidal activity; TDM, therapeutic drug monitoring; SAR, structure-activity relationship; MIC, minimal inhibitory concentration; $T_{1/2}$, half time; BBB, blood-brain barrier; PAMPA, parallel artificial membrane permeation assay; DSBs, double stranded breaks; FLC, fluconazole; DMF, dimethylformamide; DMSO, dimethyl sulfoxide; PI, propidium iodide; KEGG, Kyoto Encyclopedia of Genes and Genomes; DEGs, differentially expressed genes; RPKM, reads per kilobase per million mapped reads; ATM, ataxia telangiectasia mutated; TFA, trifluoroacetic acid; XTT, 2,3-bis(2-hydroxyethylthio)naphthalene-1,4-dione; OD, optical density; TEM, transmission electron microscopy; SDs, standard deviations; CSH, cellular surface hydrophobicity; ICR, institute of cancer research; CFU, colony-forming units; *C. alb*., *Candida albicans*; *C. par*., *Candida parapsilosis*; *C. neo*., *Cryptococcus neoformans*; *C. gla*., *Candida glabrata*.

## REFERENCES

1. Denning, D. W.; Bromley, M. J. How to bolster the antifungal pipeline. *Science* **2015**, *347*, 1414-1416.

2. Brown, G. D.; Denning, D. W.; Levitz, S. M. Tackling human fungal infections. *Science* **2012**, *336*, 647.

3. Spitzer, M.; Robbins, N.; Wright, G. D. Combinatorial strategies for combating invasive fungal infections. *Virulence* **2017**, *8*, 169-185.

4. Sloan, D. J.; Parris, V. Cryptococcal meningitis: epidemiology and therapeutic

options. *Clin. Epidemiol.* **2014**, *6*, 169-182.

5. Liu, T. B.; Perlin, D. S.; Xue, C. Molecular mechanisms of cryptococcal meningitis. *Virulence* **2012**, *3*, 173-181.

6. Williamson, P. R.; Jarvis, J. N.; Panackal, A. A.; Fisher, M. C.; Molloy, S. F.; Loyse, A.; Harrison, T. S. Cryptococcal meningitis: epidemiology, immunology, diagnosis and therapy. *Nat. Rev. Neurol.* **2017**, *13*, 13-24.

7. Rajasingham, R.; Smith, R. M.; Park, B. J.; Jarvis, J. N.; Govender, N. P.; Chiller, T. M.; Denning, D. W.; Loyse, A.; Boulware, D. R. Global burden of disease of HIV-associated cryptococcal meningitis: an updated analysis. *Lancet Infect. Dis.* **2017**, *17*, 873-881.

8. Shaw, K. J.; Schell, W. A.; Covel, J.; Duboc, G.; Giamberardino, C.; Kapoor, M.; Moloney, M.; Soltow, Q. A.; Tenor, J. L.; Toffaletti, D. L.; Trzoss, M.; Webb, P.; Perfect, J. R. In vitro and in vivo evaluation of APX001A/APX001 and other gwt1 inhibitors against cryptococcus. *Antimicrob. Agents Chemother.* **2018**, *62*, e00523-18.

9. Ogundeji, A. O.; Porotloane, B. F.; Pohl, C. H.; Kendrekar, P. S.; Sebolai, O. M. Copper acyl salicylate has potential as an anti-cryptococcus antifungal agent. *Antimicrob. Agents Chemother.* **2018**, *62*, e02345-17.

10. Perfect, J. R. The antifungal pipeline: a reality check. *Nat. Rev. Drug Discovery* **2017**, *16*, 603-616.

11. Coelho, C.; Casadevall, A. Cryptococcal therapies and drug targets: the old, the new and the promising. *Cell. Microbiol.* **2016**, *18*, 792-799.

12. Day, J. N.; Chau, T. T.; Wolbers, M.; Mai, P. P.; Dung, N. T.; Mai, N. H.; Phu,

N. H.; Nghia, H. D.; Phong, N. D.; Thai, C. Q. Combination antifungal therapy for cryptococcal meningitis. *N. Engl. J. Med.* **2013**, *368*, 1291-1302.

13. Zhai, B.; Wu, C.; Wang, L.; Sachs, M. S.; Lin, X. The antidepressant sertraline provides a promising therapeutic option for neurotropic cryptococcal infections. *Antimicrob. Agents Chemother.* **2012**, *56*, 3758-3766.

14. Koselny, K.; Green, J.; Didone, L.; Halterman, J. P.; Fothergill, A. W.; Wiederhold, N. P.; Patterson, T. F.; Cushion, M. T.; Rappelye, C.; Wellington, M. The celecoxib derivative AR-12 has broad spectrum antifungal activity in vitro and improves the activity of fluconazole in a murine model of cryptococcosis. *Antimicrob. Agents Chemother.* **2016**, *60*, 7115-7127.

15. Gemma L. Nixon, L. M., Adam Johnson, Nicola Farrington, Sarah Whalley, Joanne Livermore, Cristien Natal, Gina Washbourn, Jaclyn Bibby, Neil Berry, Jodi Lestner, Megan Truong, Andrew Owen, David Lalloo,Ian Charles, William Hope. Repurposing and reformulation of the antiparasitic agent flubendazole for treatment of cryptococcal meningoencephalitis, a neglected fungal disease. *Antimicrob. Agents Chemother.* **2018**, *62*, e01909-17.

16. Joffe, L. S.; Schneider, R.; Lopes, W.; Azevedo, R.; Staats, C. C.; Kmetzsch, L.; Schrank, A.; Del Poeta, M.; Vainstein, M. H.; Rodrigues, M. L. The anti-helminthic compound mebendazole has multiple antifungal effects against cryptococcus neoformans. *Front. Microbiol.* **2017**, *8*, 519-535.

17. Liu, N.; Tu, J.; Dong, G.; Wang, Y.; Sheng, C. Emerging new targets for the treatment of resistant fungal infections. *J. Med. Chem.* **2018**, *61*, 5484-5511.

18. Wang, S.; Wang, Y.; Liu, W.; Liu, N.; Zhang, Y.; Dong, G.; Liu, Y.; Li, Z.; He, X.; Miao, Z.; Yao, J.; Li, J.; Zhang, W.; Sheng, C. Novel carboline derivatives as potent antifungal lead compounds: design, synthesis, and biological evaluation. *ACS Med*. *Chem*. *Lett*. **2014**, *5*, 506-511.

19. Cochrane, E. J.; Hassall, L. A.; Coldham, I. Preparation of 1-Substituted Tetrahydro-beta-carbolines by Lithiation-Substitution. *J Org Chem* 2015, 80, 5964-5969.

20. Wu, S.; Wang, Y.; Liu, N.; Dong, G.; Sheng, C. Tackling fungal resistance by biofilm inhibitors. *J*. *Med*. *Chem*. **2017**, *60*, 2193-2211.

21. Jiang, Z.; Liu, N.; Hu, D.; Dong, G.; Miao, Z.; Yao, J.; He, H.; Jiang, Y.; Zhang, W.; Wang, Y. The discovery of novel antifungal scaffolds by structural simplification of the natural product sampangine. *Chem*. *Commun*. **2015**, *51*, 14648-14651.

22. Osterholzer, J. J.; Surana, R.; Milam, J. E.; Montano, G. T.; Chen, G. H.; Sonstein, J.; Curtis, J. L.; Huffnagle, G. B.; Toews, G. B.; Olszewski, M. A. Cryptococcal urease promotes the accumulation of immature dendritic cells and a non-protective T2 immune response within the lung. *Am*. *J*. *Pathol*. **2009**, *174*, 932-943.

23. Nosanchuk, J. D.; Casadevall, A. The contribution of melanin to microbial pathogenesis. *Cell*. *Microbiol*. **2003**, *5*, 203-223.

24. Shi, M.; Li, S. S.; Zheng, C.; Jones, G. J.; Kim, K. S.; Zhou, H.; Kubes, P.; Mody, C. H. Real-time imaging of trapping and urease-dependent transmigration of Cryptococcus neoformans in mouse brain. *J*. *Clin*. *Invest*. **2010**, *120*, 1683-1693.

46

25. Xu, Y. X.; Wang, H.; Li, X. K.; Dong, S. N.; Liu, W. W.; Gong, Q.; Wang, T. D.; Tang, Y.; Zhu, J.; Li, J. Discovery of novel propargylamine-modified 4-aminoalkyl imidazole substituted pyrimidinylthiourea derivatives as multifunctional agents for the treatment of Alzheimer's disease. *Eur. J. Med. Chem.* **2018**, *143*, 33-47.

26. Xu, P.; Zhou, Z.; Xiong, M.; Zou, W.; Deng, X.; Ganaie, S. S.; Kleiboeker, S.; Peng, J.; Liu, K.; Wang, S. Parvovirus B19 NS1 protein induces cell cycle arrest at G2-phase by activating the ATR-CDC25C-CDK1 pathway. *PLoS Pathog.* **2017**, *13*, e1006266.

27. Chen, X.; Niu, H.; Yu, Y.; Wang, J.; Zhu, S.; Zhou, J.; Papusha, A.; Cui, D.; Pan, X.; Kwon, Y.; Sung, P.; Ira, G. Enrichment of Cdk1-cyclins at DNA double-strand breaks stimulates Fun30 phosphorylation and DNA end resection. *Nucleic Acids Res.* **2016**, *44*, 2742-2753.

28. Paull, T. T.; Rogakou, E. P.; Yamazaki, V.; Kirchgessner, C. U.; Gellert, M.; Bonner, W. M. A critical role for histone H2AX in recruitment of repair factors to nuclear foci after DNA damage. *Curr. Biol.* **2000**, *10*, 886-895.

29. Hour, M. J.; Liu, W. T.; Lu, I. C.; Kuo, S. C.; Gean, P. W. Aggravated DNA damage as a basis for enhanced glioma cell killing by MJ-66 in combination with minocycline. *Am. J. Cancer Res.* **2014**, *4*, 474-483.

30. Zhao, X.; Guo, Y.; Jiang, C.; Chang, Q.; Zhang, S.; Luo, T.; Zhang, B.; Jia, X.; Hung, M. C.; Dong, C.; Lin, X. JNK1 negatively controls antifungal innate immunity by suppressing CD23 expression. *Nat. Med.* **2017**, *23*, 337-346.

31. Guo, Y.; Bao, Y.; Ma, M.; Yang, W. Identification of key candidate genes and

pathways in colorectal cancer by integrated bioinformatical analysis. *Int. J. Mol. Sci.*
**2017**, *18*, E722.

32. Liang, B.; Li, C.; Zhao, J. Identification of key pathways and genes in colorectal
cancer using bioinformatics analysis. *Med. Oncol.* **2016**, *33*, 111.

33. Li, W. R.; Shi, Q. S.; Dai, H. Q.; Liang, Q.; Xie, X. B.; Huang, X. M.; Zhao, G.
Z.; Zhang, L. X. Antifungal activity, kinetics and molecular mechanism of action of
garlic oil against candida albicans. *Sci. Rep.* **2016**, *6*, 22805.

34. Colangelo, T.; Polcaro, G.; Ziccardi, P.; Pucci, B.; Muccillo, L.; Galgani, M.;
Fucci, A.; Milone, M. R.; Budillon, A.; Santopaolo, M.; Votino, C.; Pancione, M.;
Piepoli, A.; Mazzoccoli, G.; Binaschi, M.; Bigioni, M.; Maggi, C. A.; Fassan, M.;
Laudanna, C.; Matarese, G.; Sabatino, L.; Colantuoni, V. Proteomic screening
identifies calreticulin as a miR-27a direct target repressing MHC class I cell surface
exposure in colorectal cancer. *Cell Death Dis.* **2016**, *7*, e2120.

35. Wang, S.; Wang, Y.; Liu, W.; Liu, N.; Zhang, Y.; Dong, G.; Liu, Y.; Li, Z.; He,
X.; Miao, Z. Novel carboline derivatives as potent antifungal leadcompounds: design,
synthesis, and biological evaluation. *ACS Med. Chem. Lett.* **2014**, *5*, 506-511.

36. Liu, N.; Zhong, H.; Tu, J.; Jiang, Z.; Jiang, Y.; Jiang, Y.; Jiang, Y.; Li, J.; Zhang,
W.; Wang, Y. Discovery of simplified sampangine derivatives as novel fungal biofilm
inhibitors. *Eur. J. Med. Chem.* **2017**, *143*, 1510-1523.

37. Uribe, C. C.; Dos, S. d. O. F.; Grossmann, B.; Kretzmann, N. A.; Reverbel, d. S.
T.; Giugliani, R.; Matte, U. Cytotoxic effect of amphotericin B in a myofibroblast cell
line. *Toxicol. In Vitro* **2013**, *27*, 2105-2109.

38. Rosenberg, M. Microbial adhesion to hydrocarbons: twenty‐five years of doing MATH. *Fems Microbiol. Lett.* **2006**, *262*, 129-134.

39. Di, L.; Kerns, E. H.; Fan, K.; Mcconnell, O. J.; Carter, G. T. High throughput artificial membrane permeability assay for blood–brain barrier. *Eur. J. Med. Chem.* **2003**, *38*, 223-232.

40. Li, D. D. Fluconazole assists berberine to kill fluconazole-resistant candida albicans. *Antimicrob. Agents Chemother.* **2013**, *57*, 6016-6027.

41. Montès, B.; Mallié, M.; Jouvert, S.; Bastide, J. M. Morphological changes of Candida, albicans induced by saperconazole. *Mycoses* **1991**, *34*, 287-292.

1
2
3
4
5
6
7
8
9
10
11
12
13
14
15
16
17
18
19
20
21
22
23
24
25
26
27
28
29
30
31
32
33
34
35
36
37
38
39
40
41
42
43
44
45
46
47
48
49
50
51
52
53
54
55
56
57
58
59
60

# Table of Contents Graphic